

Department of Electrical Engineering and Electronics, UMIST

Fourth Year Project Final Report

High Power Gunn Diode Oscillators

Michael Gaskill
David Headland
Jamie Higginbotham
Ruth Irwin
Andrew Nelms
Raymond Wan

Supervisors:
Dr. R Sloan
Dr. WS Truscott

A report submitted in partial fulfilment of the requirements of
MEng degrees in the Department of Electrical Engineering and
Electronics

21st April 2004

Contents

Contents	i
List of figures	v
1 Executive Summary	1
2 Introduction	3
2.1 Report summaries	3
2.2 History and research	3
2.3 Changes since the interim report	6
3 Management	8
3.1 General management	8
3.1.1 Managerial roles	8
3.1.2 Meetings and issues	9
3.1.3 Document management and circulation	10
3.1.4 Communication with e2v Technologies	10
3.2 Health and safety	11
3.3 Auditing	11
3.4 Web site	12
4 Single Gunn diode oscillator	14
4.1 Design	14
4.1.1 Introduction	14

4.1.2	Re-addressing the single Gunn diode oscillator	15
4.1.3	Power losses	20
4.1.4	Quality factor	23
4.1.5	Summary	26
4.2	Radial line transformer	26
4.2.1	Introduction	26
4.2.2	Filter circuit	28
4.2.3	Advanced Design System (ADS)	30
4.2.4	High Frequency Structure Simulator	32
4.2.5	Filter with two capacitors	36
4.2.6	Resonant disc	37
4.2.7	Gunn diode model	44
4.2.8	Future work	44
4.2.9	Summary	45
4.3	Testing	45
4.3.1	Introduction	45
4.3.2	Device set up and e2v test rig	46
4.3.3	UMIST test rig	47
4.3.4	Test result analysis	52
4.3.5	Summary	53
5	Multiple Gunn diode oscillator	55
5.1	Design	55
5.1.1	Introduction	55
5.1.2	Multiple device oscillator design	55
5.1.3	Backshort	58
5.1.4	Building progress	58
5.1.5	Summary	59
5.2	Radial line transformer	59
5.3	Power supply	59

5.3.1	Introduction	59
5.3.2	Power supply requirements	60
5.3.3	Data acquisition board	61
5.3.4	Sample and hold	62
5.3.5	Demultiplexer	63
5.3.6	Inverting amplifier	64
5.3.7	Buffer	64
5.3.8	Voltage regulator	65
5.3.9	LabView	71
5.3.10	Summary	75
6	Conclusions	76
6.1	Progress to date	76
6.2	Future objectives for this design	77
6.2.1	Simulation of the backshort	78
6.2.2	Simulation of the diode position	78
6.2.3	Alternate waveguide designs	78
6.2.4	Power combining more Gunn diodes	79
6.2.5	Power combining at non-fundamental harmonics	79
7	Future work	80
7.1	Hot electron injection	80
7.1.1	Reasons for hot electron injection	80
7.1.2	Experimental results	81
A	Electronic information	82
A.1	Project plan	83
A.2	Records of the meetings	83
A.3	Financial accounts	83
A.4	Presentation slides	83
A.5	PHP source	83

A.6	Technical drawings	84
A.7	Issues log	84
A.8	Experimental results	84
A.9	Communications log	84
A.10	Power supply	84
A.11	Main reports	84
	Bibliography	85

List of Figures

2.1	Overview of the interim report	4
2.2	Overview of the final report	4
3.1	Time/cost/quality triangle (Reiss 2001)	12
4.1	External components of the single device oscillator	14
4.2	Gunn diode housing	17
4.3	Dimensions of the circular waveguide (Pozar 1998)	19
4.4	Frequency vs. backshort distance	20
4.5	Circular variable backshort	21
4.6	Attenuation vs frequency of the three components	24
4.7	Radial line transformer in the waveguide cavity	27
4.8	Filter circuit components	28
4.9	Coaxial line dimensions: (a) Capacitor, (b) Inductor	30
4.10	Screenshot of components from ADS	31
4.11	S-parameter plot of filter circuit with components from ADS	32
4.12	Screenshot of coaxial lines from ADS	33
4.13	S-parameter plot of filter circuit with coaxial line from ADS	33
4.14	Screenshot of filter design from HFSS	34
4.15	S-parameter plot from HFSS of original design	35
4.16	S-parameter plot from HFSS of reduced radius design	36
4.17	New filter circuit components	36
4.18	S-parameter plot: two capacitor filter with components (ADS)	37

4.19	S-parameter plot: two capacitor filter with coax line (ADS) . . .	38
4.20	Half a resonant disc in the waveguide	39
4.21	Frequency against angle for half a resonant disc	39
4.22	Frequency against angle for smaller half resonant disc	40
4.23	Frequency against angle for half resonant disc at 1.9mm	41
4.24	Full resonant disc in the waveguide	41
4.25	Frequency against angle for full resonant disc	42
4.26	The two modes on the wave port	43
4.27	Magnitude plot for wave ports with two modes	43
4.28	Test setup at e2v Technologies	46
4.29	Graphs from e2v testing (1/2)	47
4.30	Test setup at UMIST	48
4.31	Results of testing with a 1.0 mm backshort notch	50
4.32	Results of testing with no backshort notch	51
4.33	Biasing effects	52
5.1	External components of the multiple device oscillator	56
5.2	In-line three diode combiner	57
5.3	Gunn diode housing (Barth 1981)	58
5.4	Hardware overview	61
5.5	Sample and hold amplifier	63
5.6	Line decoder logic	64
5.7	Inverting amplifier	65
5.8	Voltage follower	65
5.9	723 Regulator	66
5.10	Setup of the 723 voltage regulator	67
5.11	Thermal circuit of the pass transistor under fault conditions	68
5.12	Four output regulator	70
5.13	Initial program	72
5.14	Increment VI	73
5.15	Revised program	74
5.16	Instrument panel	74

Chapter 1

Executive Summary

The aim of the project is to power combine four Gunn diodes to create a Gunn oscillator system, which produces an output of 100 mW at 87 GHz. A Gunn diode is a device that produces a radio frequency (RF) output signal when biased with a DC voltage. Gunn diodes have low efficiency, generally about 2%, when converting from DC to RF, so the output is a low power signal, about 30 mW. To increase the magnitude of the RF output power a number of Gunn diodes (from this point onwards they may be referred to as diodes or devices) are being combined using a technology known as power combining.

The project is a collaboration with e2v Technologies, a RF technology company. e2v is sponsoring the project because they use Gunn diodes in many of their systems, and are also interested in the research to optimise the performance of Gunn diode systems. e2v has given direction to the project, as well as offering explanations, expertise and use of its manufacturing and testing facilities.

The output signal is required to be 87 GHz because the intention is that Gunn diodes will be used in terahertz imaging systems. Terahertz imaging systems operate at 260 GHz. Some research groups have undertaken studies to investigate the method of frequency multiplying to achieve the desired frequency as a multiple of an initial frequency, 260 GHz from 87 GHz.

The project has two objectives; the first is to design and build a Gunn oscillator system consisting of one Gunn diode, and the second is to use this first system to design and build a Gunn oscillator system with multiple diodes and employ power combining. To achieve these objectives there are many tasks, including researching and understanding Gunn diodes, waveguides,

power combining, and designing, simulating and building the Gunn diode oscillator.

In the interim report, a summary of the Gunn diode was given, research on different types of Gunn diode housing was completed and a waveguide design for the single Gunn diode system (or single device oscillator) was summarised and submitted to the workshop in UMIST. Simulation work on the waveguide and the Gunn diode components was begun.

Since the completion of the interim report, the UMIST workshop returned the single Gunn diode system design; the workshop was incapable of making the system because the required tolerances were too high. After further delay e2v Technologies took the design and recently completed the manufacture of the system. The system is now being tested, with preliminary tests showing the system oscillates at around 85 GHz with a power output of 55 mW. The multiple Gunn diode system design has been completed and submitted to e2v and should be manufactured and ready to test by May.

Due to the problems and delays with the UMIST workshop, the manufacture of the multiple Gunn diode system is four weeks behind the time plan. Because of the delays, the order of work has been rearranged and additional time has been spent using the simulation tools and researching alternative Gunn diode technologies and routes for possible further work.

Chapter 2

Introduction

2.1 Report summaries

An extensive part of this project is research and this research is summarised in the interim report. The research is broken down into three areas: the Gunn diode, Gunn diode housing and power combining, as illustrated in figure 2.1. From the three areas of research the design for the single Gunn diode oscillator was created, this design is included in the interim report.

The overview of the Final Report is given in figure 2.2. The final report focuses on the alterations to the single diode oscillator and its testing, as well as the design and manufacture of the multiple Gunn diode oscillator. This multiple diode oscillator is the aim of the project: to build and test a Gunn diode oscillator that consists of four diodes and oscillates at 87 GHz with 100 mW of power.

2.2 History and research

The concept of a negative differential resistance region of a material due to inter-valley charge carrier transfer was first suggested by C Hilsum. Assuming that this could happen in semiconductor materials, BK Ridley and TB Watkins were the first to theorise that high field domains could form and propagate as a result of the negative differential resistance region. Together, they were able to show that the electron velocity in materials such as GaAs and InP would decrease as the electric field increased. This would only happen when the applied field strength rose above a certain value required; that required for the transition of electrons in to higher energy satellite valleys.

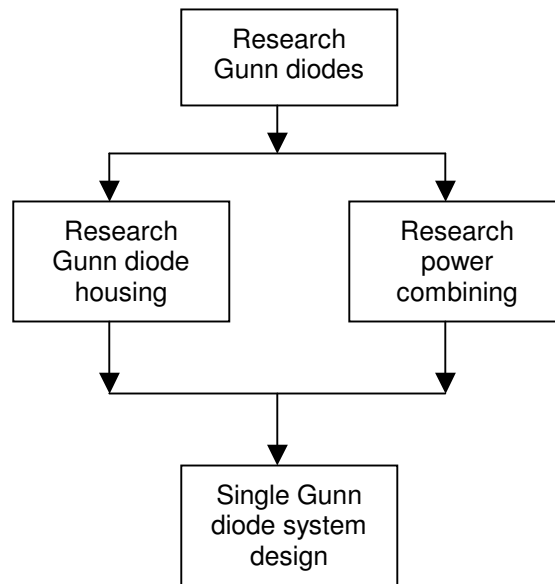


Figure 2.1: Overview of the interim report

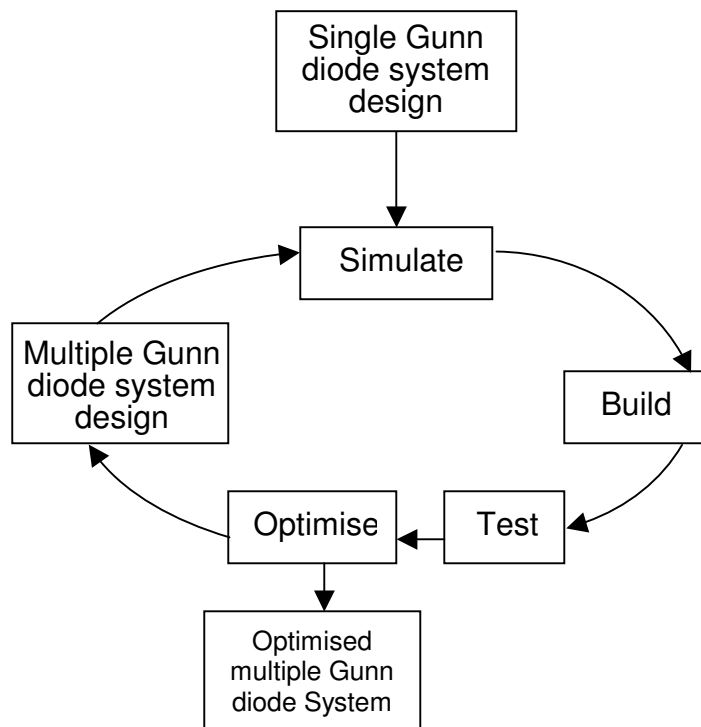


Figure 2.2: Overview of the final report

In 1963, John Gunn started a study into the voltage-current characteristics of samples of GaAs and InP semiconductors whilst working for IBM. He discovered that spontaneous microwave oscillations occurred when the electric field applied to the device was increased over a certain threshold, 3 kV cm^{-1} for GaAs and 6 kV cm^{-1} for InP. He went on to find that the high field domains predicted by Ridley, Watkins and Hilsum were responsible for this, with the domain forming near the cathode, propagating across the device and ending at the anode. The process would then repeat.

As the domains formed, he found that the current would drop, and then would rise sharply as the domains were annihilated (Gunn 1963). This phenomenon is now known as the Gunn effect, although it was not until 1964 that Herbert Kroemer explained the effect by linking it to Ridley, Watkins and Hilsum's research.

The discovery of the Gunn effect prompted a lot of research into compound semiconductors such as GaAs. The first workshop on compound semiconductor microwave devices was opened by Lester Eastman in New York in 1965 to discuss the progress in this new field of research. A similar group was set up in Europe, and is still running today as WOCSDICE, the Workshop on Compound Semiconductor Devices and Integrated Circuits held in Europe.

Part of the active area of a Gunn diode is used as the electrons gain enough energy to transfer to the satellite valleys. This presents limitations on the maximum usable frequency and the maximum RF power output of the devices because a dead zone is created at the start of the active area. A lot of work was put into finding ways of reducing the dead zone (Ferry & Grondin 1985).

Various methods were suggested for reducing the length of the dead zone, mainly concentrating on creating large electric fields to excite electrons before they enter the active area. Planar doped barriers and graded gaps placed between the cathode and the active areas were found to help enormously. These methods resulted in the electrons being raised to satellite energy valleys before entering the active area, so the methods are collectively referred to as hot electron injection. Such devices were available commercially by 1984.

By the 1980s, many people had started to look at more exotic semiconductor materials than GaAs. Materials such as InP and GaN have much larger band gaps than GaAs, promising higher frequencies of operation with higher RF power outputs. The technology for working with these materials was not as advanced as for GaAs, however, and InP has recently been determined unsuitable for large-scale commercial applications.

Research is now turning back to pushing the performance of GaAs devices

further since InP has been determined unsuitable. Research is being done into the makeup of individual devices and into the device arrangement in systems, for example placing multiple transit regions into a single diode arrangement, and in multiple device system, such as power combining and extracting non-fundamental frequencies, as is the aim of this project.

2.3 Changes since the interim report

The manufacturing aspect of this project has been very time consuming, about 16 weeks in total. At the start of the project this was identified as an area that could slow other parts of the project down. To reduce this potential setback the team approached outside manufacturers, but using other manufacturers would result in a significant increase in the project costs and proved to be unfeasible.

In the interim report it was stated that the designs had been submitted to the UMIST workshop facilities with the intention of having the single device oscillator completed by mid-January. Due to a shortage of skilled machinists this proved to be impractical, therefore e2v intervened and offered to manufacture the components. The initial plan was to have the single device oscillator manufactured by the start of March. This has since been extended to the end of March.

A recent visit to e2v resulted in the single device oscillator being completed and it is now with the testing team for analysis. Due to the workload on e2v, minor modifications have had to be made to the design since the original design was submitted, although the basic principles remain the same. The modifications are: The backshort is now circular and allows for tuning of the second harmonic. e2v have also suggested that the multiple device oscillator should consist of three instead of four Gunn diodes. The multiple device oscillator will utilise two components from the single device oscillator (the backshort and the second harmonic waveguide), therefore the components being manufactured by e2v are reduced to only the three Gunn diode housings. The intention is to have these components ready for the first week in May, allowing adequate time for testing.

The building sections of the report (sections 4.1 and 5.1) explains the problems that have been encountered and how they have been solved.

As a result of the manufacturing problems, the testing on the multiple device oscillator that was planned for between Christmas and Easter has been moved

back to May, and the testing of the single device oscillator has been shifted to the beginning of April, the first week of the Easter break.

The plan is to complete all testing and tuning that was originally planned, but we may have time only to recommend future changes rather than implementing them in the device. This has been agreed with e2v as a new objective.

Chapter 3

Management

3.1 General management

The team have introduced a number of practices to coordinate the project and team. Practices have been instigated in the areas of sharing managerial duties, inter-team meetings and issue solving, methods to communicate, circulate and file documentation, and to communicate with e2v.

3.1.1 Managerial roles

The managerial duties were split into three roles: manager, secretary and auditor. At the beginning of the project, the team nominated candidates for each role and the appointment of roles were voted upon. Due to the success of the system the roles have remained with the same members throughout the project.

The duties of the Manager are to:

- Create and maintain the project plan.
- Deliver reports to the 4th year tutor.
- Interface between the team and the 4th year tutor.
- Arbitrate on contentious issues.
- Manage the team members — monitoring and encouraging.
- Interface between the team and the sponsor e2v Technologies.

- Record all communications with e2v Technologies.
- Check all documents for consistency and errors.

The duties of the Secretary are to:

- Arrange and circulate the agenda for meetings.
- Record the minutes of meetings and circulate them.
- Organise the presentation and demonstration.
- Ensure logbooks are well maintained.
- Create and maintain the website and mailing lists.
- Maintain an Issues Log.

The duties of the Auditor are to:

- Set up and maintain a record of costs
- Organise and maintain document management
- Produce Risk Assessments for the team
- Supervise closure at the end of the project

3.1.2 Meetings and issues

The team meets weekly for a formal project meeting to discuss individual progress, offer each other support and resolve any issues. As well as the formal meeting team members regularly work together to complete tasks. Agendas are created for each meeting and circulated about a week beforehand. Minutes are kept during the meeting and circulated immediately afterwards. An Issues Log has been created and all ongoing issues are recorded in the log and changes or updates to the issue status are recorded. The Issues Log is in appendix A.7.

3.1.3 Document management and circulation

All documentation, including research documents, reports, minutes and agendas are filed, managed and circulated in a number of ways. The first way is that a hard copy of the document is placed in one of three files: the research file, team documentation file or management file. Research documents are placed in the research file with a one-page summary outlining any points of interest in the document; this file is maintained in alphabetical order of the author. Reports and documents written by the team are placed in the team documentation file in date order. Minutes and agendas are placed in the management file in date order. These three files are kept in the project room.

The second way of filing documents is an electronic copy is placed on the project website, this enables all documentation to be circulated to all of the team. Similarly to the hard copies, there are different locations where different types of documents are placed; the “useful links” section is for research documents, “formal documentation” section is for team documents and “meetings” sections is for minutes and agendas. A copy of all documentation is given to the secretary who places it on the website and posts a message to the team mailing list to inform the team of the newly available documents.

The website has proved particularly useful, enabling the team to access any of the documents from any location. The minutes and agenda are always placed on the website promptly after each meeting. Supporting the website there are a number of mailing lists, the first and main list which includes the six members of the team, a second list which includes the members of the team and the project supervisors and a third list which includes the members of the team, the supervisors and e2v Technologies.

3.1.4 Communication with e2v Technologies

e2v Technologies are sponsoring the project, and have given direction to the project as well as offering expertise and use of their manufacturing and testing facilities. The relationship with e2v is that they act as our customer, so the aim is that e2v are approached competently, only when necessary. To achieve and maintain this professional relationship, a team member, the manager, was delegated the role of liaising with e2v on behalf of the team. Communication with e2v has been limited to a maximum of two communications a week. If a team member needs to speak with e2v, they first have to seek agreement from the team manager and a log of all communications has been maintained. This log can be found in appendix A.9.

3.2 Health and safety

As part of the team's commitment to working safely, any contentious issues have been dealt with by implementing a risk assessment for each task. This system has worked well, and at the present time there are no reportable injuries due accidents or incidents with project work.

One of the main reasons for completing a risk assessment is to identify and eliminate any risks, this is needed to keep all hazards to a minimum. The result of one assessment was that the power supply for the multiple device oscillator required testing. It was decided that a Portable Appliance Test (PAT) would be completed. The successful completion of this test ensures that the device is in good working order and safe enough to be plugged into a domestic supply (The Electricity at Work Regulations 1989).

Since the interim report, safety has been an area requiring little development. The risk assessment system highlighted the most potential dangers in the various activities. Following the guidelines seen in appendix B of the interim report should ensure that no accidents will occur through the remainder of this project.

3.3 Auditing

This project has three management objectives which must be monitored throughout the project, as are illustrated in figure 3.1.

The correct value of each objective must be found for the triangle to balance. The time period for the project is two semesters, and was defined at the beginning of the project. The length of the project could not be altered so a stringent time plan was generated. The remaining items on the triangle are cost and quality. Quality does not mean good or bad, it is about completing the project in accordance with the initial requirements, laid down in the project specification. Therefore cost is the variable that needs constant monitoring for the project to balance.

The financial elements to this project have been substantially reduced with the assistance of e2v in the manufacturing of the devices.

Appendix A.3 contains a copy of the financial summary of the project. The financial summary looks into the full costs of the design and manufacture of the systems. The project costs include three key figures, the first is the capital spent on the oscillators, which came to approximately £422.83. A

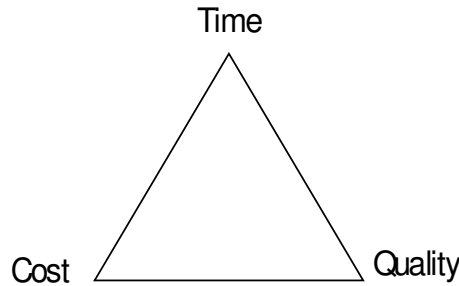


Figure 3.1: Time/cost/quality triangle (Reiss 2001)

considerable amount of this figure is the cost of the flanges from Flann. These were required for making accurate measurements during testing. Excluding the flanges, the final cost would be £222.83, which is remarkably low for this type of apparatus. Also included in this figure are materials including the Gunn diodes and brass, which were provided by e2v and if excluded would reduce this figure even further.

The second cost takes into account all the money spent on additional resources including miscellaneous equipment and costs such as stationary and travel expenses. These resources were essential for first-class management of the project.

The final cost includes the approximate full cost with man-hours included. This cost includes an educated guess for the rate of pay of students and use of facilities. The final figure came to £6 604.28, which is extremely reasonable for six months of development work. A project of this nature could be expected to cost around £10000.

3.4 Web site

The project web site has proved to be an invaluable management tool throughout the duration of this project. It not only allows finished documents to be quickly made publicly available, but also allows for all communications between the group members to be archived. All mailing list traffic, minutes and agendas are archived, as well as all time plans. The web site is particularly invaluable because it allows reference access from any web-based terminal in the world.

The information provided on the web site is of interest to many third parties.

In February 2004, the team was contacted by a student at a Greek university interested in our work. He had found our web site listed on a search engine. The team have observed, by analysis of the web site logs, an average of 106 unique hosts visit the project web site every week. The number of unique visitors is more difficult to establish, as NAT, proxies and dynamic IP addresses will affect these statistics.

The basic web site set-up has changed little this semester, and the description given in section 3.13 in the interim report is still valid. The main changes since that report are discussed here:

- Move to version 1.3.29 of the Apache web server to avoid potential security problems with the earlier versions.
- Change of Linux kernel on the server from 2.4.21 to 2.6.5 to benefit from a much improved SMP scheduler. This should allow heavier loads to be dealt with without as much slowdown by balancing all tasks across the available processors more effectively and efficiently.
- IPv6 provision of the web site, in an effort to assist the migration of Internet services to the new protocol. The DNS has been updated with AAAA records so that IPv6 clients should automatically use IPv6 connections, whereas IPv4 clients or networks will not lose any functionality. The web site is connected to the UK6x IPv6 backbone.

Chapter 4

Single Gunn diode oscillator

4.1 Design

4.1.1 Introduction

Up to December the building element of this project was productive and on time, the exception was having the single device oscillator built by mid-January, and having the multiple device oscillator designs submitted before Easter. It was found that there were few manufacturers able to build these devices to the required specification, this factor was identified as the bottleneck risk at the start of the project. Therefore e2v technologies have been relied on to manufacture all components.

Slight modifications have been made since the original design was completed and presented in the interim report, although the basic principle remains the same. The most visible alteration is that a circular backshort component composed of two backshorts has been added to the design. This alteration gives additional tunability when altering the second harmonic frequency. The flow diagram shown in figure 4.1 details how the components will now fit together.

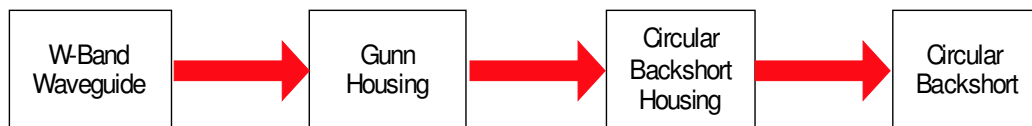


Figure 4.1: External components of the single device oscillator

The aim of this section, 4.1, is to review the theory of the single device oscillator, the modifications and a consideration of the potential losses that will occur.

4.1.2 Re-addressing the single Gunn diode oscillator

All pieces of the system will be manufactured in brass to a set tolerance of ± 0.02 mm.

4.1.2.1 2nd Harmonic Waveguide

The output waveguide remains as originally designed. It allows the second harmonic frequency to pass through it and out, and reflects the fundamental harmonic back into the waveguide.

4.1.2.2 Gunn diode housing

The Gunn diode housing is still part of the fundamental waveguide cavity. Most of the dimensions for the fundamental frequency waveguide are unchanged, but the length needs to be re-calculated. The length can be calculated by re-addressing the equations seen in section 3.12.4 of the interim report, this yields equations 4.1 to 4.3:

$$\begin{aligned}\lambda_0 &= \frac{c}{f_0} \\ \lambda_0 &= \frac{3 \times 10^8}{43.5 \times 10^9} \\ \lambda_0 &= 6.90 \text{ mm}\end{aligned}\tag{4.1}$$

$$\begin{aligned}\lambda_c &= 2\sqrt{\frac{2}{5}}\lambda_0 \\ \lambda_c &= 1.26 \times 6.90 \\ \lambda_c &= 8.72 \text{ mm}\end{aligned}\tag{4.2}$$

$$\begin{aligned}\lambda_c &= 2a \\ a &= 4.36 \text{ mm}\end{aligned}\tag{4.3}$$

Where:

λ_c Cut-off wavelength.

λ_0	Fundamental wavelength.
λ_g	Guide wavelength.
a	Waveguide width.
c	Velocity of light in free space.

This dimension a is slightly different from the original value ($a = 3.95$ mm) given in the interim report, this is with reference to Barth's theory. This new value of a alters the waveguide width to 4.36 mm (Barth 1981). The cut-off frequency is given by given by equation 4.4:

$$\begin{aligned}
 f_c &= \frac{c}{\lambda_c} \\
 &= \frac{3 \times 10^8}{2 \times 4.36 \times 10^{-3}} \\
 f_c &= 34.4 \text{ GHz}
 \end{aligned} \tag{4.4}$$

Therefore, below the frequency of 34.4 GHz the wave will not propagate inside the waveguide. Once the wavenumber, k , is found the length of the diode housing can be calculated as follows:

$$\begin{aligned}
 k &= \frac{2\pi f_0 \sqrt{\epsilon_r}}{c} \\
 &= \frac{2\pi 43.5 \times 10^9}{3 \times 10^8} \\
 k &= 911.06 \text{ m}^{-1}
 \end{aligned} \tag{4.5}$$

$$\begin{aligned}
 \lambda_g &= \frac{l\pi}{\sqrt{k^2 - \left(\frac{\pi}{a}\right)^2}} \\
 &= \frac{2\pi}{\sqrt{911.06^2 - \left(\frac{\pi}{4.36 \times 10^{-3}}\right)^2}} \\
 \lambda_g &= 11.26 \text{ mm}
 \end{aligned} \tag{4.6}$$

The diode mounting will be approximately $\frac{\lambda_g}{2}$ (Barth 1981), therefore the diode will be mounted exactly in the middle of the housing at 5.63 mm.

The mounting of the Gunn diode and radial line transformer is a complex task within itself. The Gunn diode is mounted within a casing, which acts as a heatsink and dissipates the heat to the brass walls of the waveguide. This

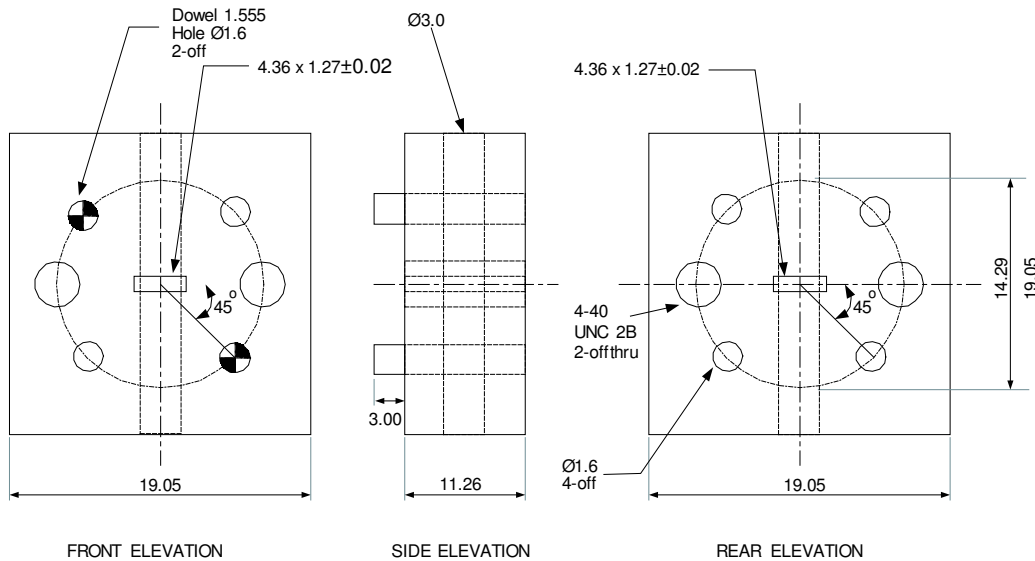


Figure 4.2: Gunn diode housing

heatsink casing is then screwed into a 3 mm hole so the Gunn diode sits just above the waveguide surface with the casing flush to this waveguide surface. The position of the casing can be altered when the oscillator is being tested, this can optimise the overall system performance.

Additionally, the radial line transformer is spring mounted on the top of the Gunn diode by a composition of washers. A modest amount of pressure is required on this spring so that the position of the radial line transformer and the diode is not affected by any external vibrations. The pressure is also needed since the oscillator warms up and may result in the spring expanding. Figure 4.2 shows a mechanical drawing of the Gunn diode housing.

4.1.2.3 Backshort Cavity

In the original design, a simple rectangular backshort is used; the updated design has a double circular backshort. The reason for using a circular backshort is that it will allow both the fundamental and second harmonic to be tuned, the rectangular alternative is not as flexible. The circular backshort calculations are very similar to the rectangular backshort calculations, but the cylindrical co-ordinate system is used.

Waves propagating in a waveguide are characterised by the transversal field distribution. The wave of a given transversal field distribution is denoted as

a given mode of a wave. The dominant mode in circular waveguide is TE₁₁, this mode gives the lowest possible cut-off frequency.

The size of the circular backshort is calculated using standard circular waveguide theory. The fundamental cut-off wavelength can be calculated using equation 4.7:

$$\begin{aligned}\lambda_c &= \frac{c}{f_0} \\ &= \frac{3 \times 10^8}{43.5 \times 10^9} \\ \lambda_c &= 6.89 \text{ mm}\end{aligned}\tag{4.7}$$

Where:

λ_c Fundamental cut off wavelength.

c Velocity of light in free space.

f_0 Fundamental frequency.

Using this theory we find $\lambda_c = 6.89 \text{ mm}$. Now the wave number, k , can be calculated using equation 4.8:

$$\begin{aligned}k &= \frac{2\pi}{\lambda_c} \\ &= \frac{2\pi}{0.00689} \\ k &= 911.06 \text{ m}^{-1}\end{aligned}\tag{4.8}$$

From this, the dimensions of the backshort as seen in figure 4.3 can be calculated.

Knowing that $d = 2a$ and $P_{11} = 1.841$ for TE₁₁ circular waveguide, we can find d using equations 4.9 to 4.12:

$$f_0 = \frac{c}{2\pi} \sqrt{\left(\frac{P_{11}}{a}\right)^2 + \left(\frac{\pi}{d}\right)^2}\tag{4.9}$$

$$f_0 = \frac{c}{2\pi} \sqrt{\left(\frac{P_{11}}{a}\right)^2 + \left(\frac{\pi}{2a}\right)^2}\tag{4.10}$$

$$a = \frac{\sqrt{P_{11}^2 + \left(\frac{\pi}{2}\right)^2}}{k}$$

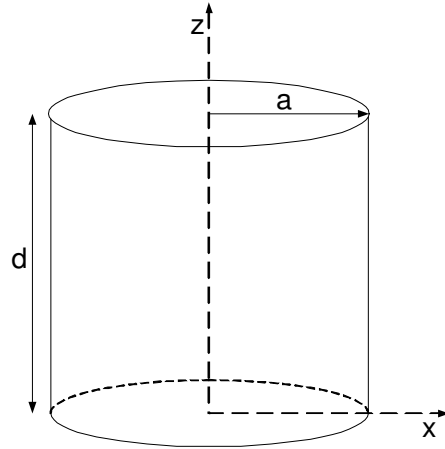


Figure 4.3: Dimensions of the circular waveguide (Pozar 1998)

$$\begin{aligned}
 &= \frac{\sqrt{1.841^2 + \left(\frac{\pi}{2}\right)^2}}{911.062} \\
 a &= 2.65 \text{ mm} \tag{4.11}
 \end{aligned}$$

$$\begin{aligned}
 d &= 2a \\
 &= 2 \times 2.656 \\
 d &= 5.31 \text{ mm} \tag{4.12}
 \end{aligned}$$

Dimension d is dependant on the position of the backshort and can be mechanically tuned thus altering the frequency. In theory the optimal performance at the required frequency will be obtained when $d = 5.31$ mm. Due to imperfections in the manufacturing of the waveguide and the surface roughness, the practical value of d may not be equal to the theoretical value. Figure 4.4 shows a plot of how the frequency is expected to vary as backshort distance d is varied. It can be seen that as the distance d increases, i.e. as the backshort is slid out, the operating frequency is reduced. A point to consider is; why is the backshort required if having no backshort will give the highest frequency? The reason for the backshort is to give some mechanical tuning to the device so the required frequency can be obtained.

With these calculations a design for the single diode device circular backshort can be completed. One of the design requirements for this component was that it should be suitable to be used as part of the multiple Gunn device. This was suggested so that in the event of any problems with the manufacture of the multiple device this component could be used again. Figure 4.5 shows

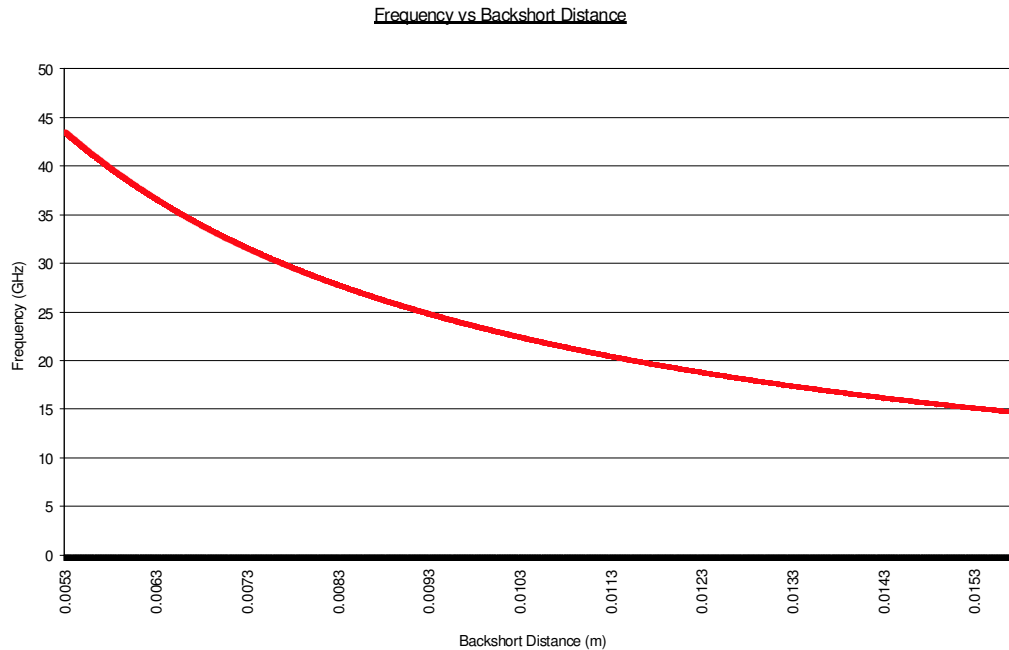


Figure 4.4: Frequency vs. backshort distance

a mechanical diagram of this component.

The second piece of this backshort component is the inner backshort, this is a brass rod which is machined to a very close tolerance so it can fit tightly into the cavity. Any gaps in the construction will result in losses. Barth's paper suggested that a second backshort can be embedded inside the fundamental backshort. The result is it will make the second harmonic output more tunable (Barth 1981). Using the similar theory to the fundamental backshort the diameter of the second harmonic waveguide is $2a = 2.65$ mm.

4.1.3 Power losses

It is a normal and relatively well known fact that waveguide systems are operated in a frequency range that ensures that only the lowest mode can propagate. If several modes can propagate simultaneously, there is no control over which mode will be carrying the transmitted signal. This may cause undue amounts of dispersion, distortion and erratic operation.

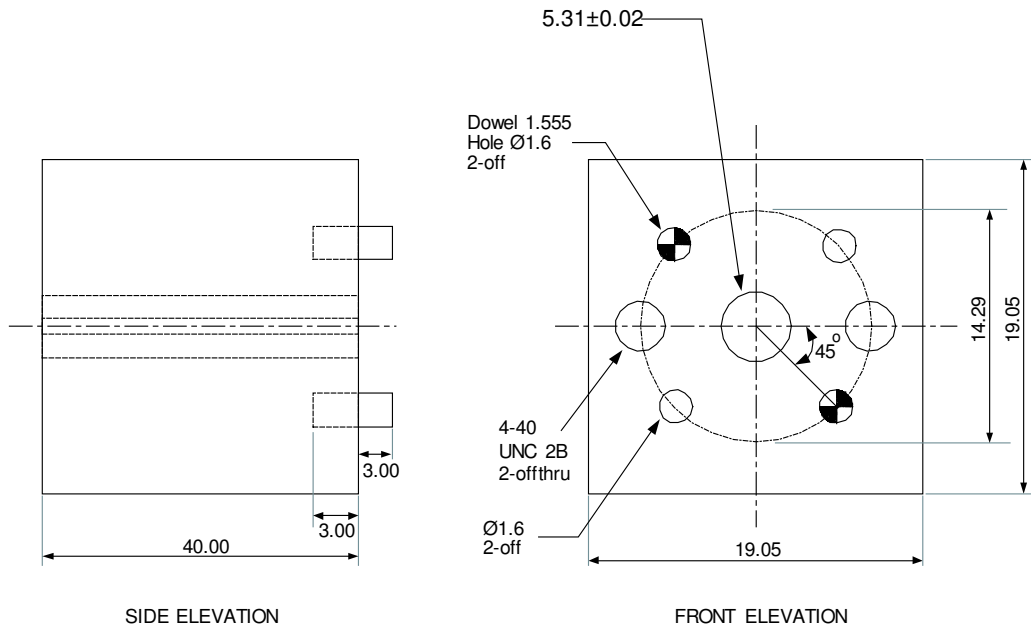


Figure 4.5: Circular variable backshort

4.1.3.1 Attenuation

In practice, all waveguides have losses due to the material of the waveguide having finite conductivity or the lossy dielectric, but usually the losses are small. These losses are usually neglected, but are calculated here to gain a sense of the quantity of attenuation that can occur in this oscillator.

Attenuation is the decrease in intensity of a signal as a result of absorption and scattering of energy. As stated above, attenuation in a waveguide can occur because of dielectric losses and conductor losses. The dielectric is air, so the losses due to the dielectric will be negligible and only conductor losses may be significant.

The main tradeoff in this waveguide system is frequency against waveguide size. As the operating frequency increases, the dimensions of the waveguide must decrease in order to maintain the operating band. The decrease in the waveguide size results in the attenuation being increasing and the transmitted power decreasing, since it is proportional to the waveguide area. All three components (waveguide, diode housing and backshort) can be considered in turn to calculate the attenuation, using standard microwave engineering

techniques. The Gunn diode housing is calculated firstly, as in equation 4.13:

$$\begin{aligned}
 \alpha_{c2} &= \frac{R_s (2b\pi^2 + a^3k^2)}{a^3b\beta k\eta} \\
 &= \frac{0.0818 (2(1.27 \times 10^{-3})\pi^2 + (4.36 \times 10^{-3})^3 \times 911.06^2)}{(4.36 \times 10^{-3})^3 1.27 \times 10^{-3} \times 557.533 \times 911.06 \times 377} \\
 &= 4.058 \times 0.09386 \\
 \alpha_{c2} &= 0.38089 \text{ Np m}^{-1} \tag{4.13}
 \end{aligned}$$

Where:

R_s	Surface resistance.
a, b	Waveguide dimensions.
β	Propagation constant.
k	Wave number.
η	Intrinsic impedance.

The unit for attenuation is nepers per meter after the Latin version of the name of John Napier, who invented the logarithm, but the attenuation is also often expressed in decibels per length and can be simply converted, as in equation 4.14:

$$\begin{aligned}
 \alpha_{c2} \text{ (dB)} &= -20 \log e^{-\alpha_{c2}l} \\
 &= -20 \log e^{-0.38 \times 11.26 \times 10^{-3}} \\
 \alpha_{c2} \text{ (dB)} &= 0.03725 \text{ dB} \tag{4.14}
 \end{aligned}$$

Given this value, this was calculated assuming the waveguide walls were perfectly smooth. The actual value of the attenuation will be higher since the walls are not perfectly smooth. Looking at this value it is clear that the loss is minute ($0.03725 \text{ dB} = 0.8\%$ loss), but should be considered to support any differences in the test measurements.

Similarly, the attenuation of the second harmonic waveguide can be calculated using the second harmonic frequency of 87 GHz. The result is an attenuation loss of $0.48069 \text{ Np m}^{-1}$. The conversions into decibels is shown in equation 4.15:

$$\begin{aligned}
 \alpha_{c2} \text{ (dB)} &= -20 \log e^{-\alpha_{c1}l} \\
 &= -20 \log e^{-0.48069 \times 4.7 \times 10^{-3}} \\
 \alpha_{c2} \text{ (dB)} &= 0.019623 \text{ dB} \tag{4.15}
 \end{aligned}$$

This value is again minute and is smaller than the previous measurement, due to the overall length of the second harmonic waveguide being less. Although it was stated that the trade-off was that as the guide size decreases the attenuation increases, this would normally be the case but since this calculation is considering the second harmonic this rule is not true for this case. In a slightly different way the attenuation of the circular backshort cavity can be calculated using equation 4.16, and the value of the attenuation in decibels is calculated in equation 4.17:

$$\begin{aligned}\alpha_{c3} &= \frac{R_s \left(k_c^2 + \frac{k^2}{P_{11}^2 - 1} \right)}{ak\eta\beta} \\ &= \frac{0.0818 \left(694.717^2 + \frac{911.06^2}{1.841^2 - 1} \right)}{2.65 \times 10^{-3} \times 911.06 \times 377 \times 589.405} \\ \alpha_{c3} &= 0.1265 \text{ Np m}^{-1}\end{aligned}\tag{4.16}$$

$$\begin{aligned}\alpha_{c3} \text{ (dB)} &= -20 \log e^{-\alpha_{c3}l} \\ &= -20 \log e^{-0.1265 \times 5.31 \times 10^{-3}} \\ \alpha_{c3} \text{ (dB)} &= 0.0058 \text{ dB}\end{aligned}\tag{4.17}$$

Figure 4.6 shows the variation of the attenuation of each component over a frequency range. The graph illustrates that the circular waveguide of the backshort suffers minimal attenuation, as the calculations suggest. It also confirms that as cavity size decreases and frequency increases, the attenuation also increases which again satisfies the previous equations.

A point to note is the Gunn diode housing has the highest attenuation (0.03725 dB at 43.5 GHz) compared to the other two components, although the overall value is too small to have a significant effect on the output.

4.1.4 Quality factor

The quality factor, or Q factor, is a measure of the quality of each component. At the resonant frequency, some of the energy of the signal is stored in the system. Due to the resistance of the system, the amplitude of the signal decays. The rate of decay is dependant upon the Q factor (Holzman & Robertson 1992). Ideally, the Q factor should be large, resulting in the energy of the system decaying slowly and minimum system losses. Ideally, the Q factor should be greater than 1000. All three components will have a separate Q factor.

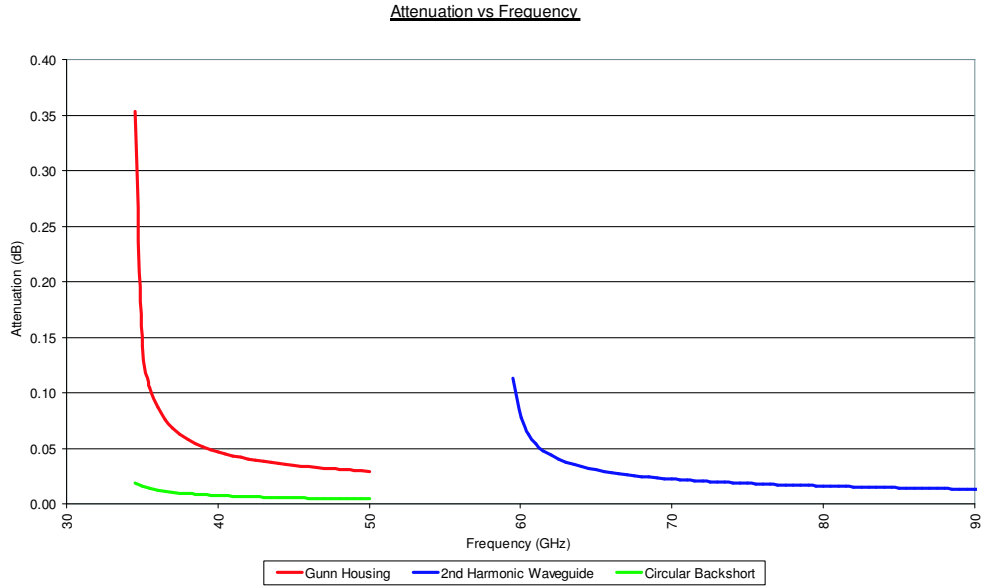


Figure 4.6: Attenuation vs frequency of the three components

The Q factor of the Gunn diode housing will be calculated first. The skin depth of the brass cavity wall, or waveguide wall, is the characteristic depth of penetration of the energy into the cavity wall. For a good conductor like brass this should be relatively small, below $0.5 \mu\text{m}$. The Q factor is inversely proportional to the skin depth. Often, the inside of a waveguide is plated with gold or silver since these materials have low skin depths, causing the Q factor to be high. In this design, this method of skin depth reduction is not used.

$$\begin{aligned}
 \delta &= \frac{\sqrt{2}}{\sqrt{\omega\mu_0\sigma}} \\
 &= \frac{\sqrt{2}}{(2\pi \times 43.5 \times 10^9)(4\pi \times 10^{-7})(2.654 \times 10^7)} \\
 \delta &= 0.4765 \times 10^{-6} \text{ m}
 \end{aligned} \tag{4.18}$$

Where:

σ Conductivity of brass ($2.654 \times 10^7 \text{ S m}^{-1}$ at 20°C).

δ Skin depth.

μ_0 Permeability of free space ($4\pi \times 10^{-7} \text{ H m}^{-1}$).

From equation 4.18, it can be concluded that most of the energy flow occurs in an extremely thin region between the surface of the waveguide wall and a depth of $0.4764 \mu\text{m}$. Using the calculated value of skin depth, the intrinsic impedance of free space can be calculated using equation 4.19:

$$\begin{aligned}\eta &= \frac{\omega\mu}{k} \\ &= \frac{2\pi(43.5 \times 10^9) \times 4\pi \times 10^{-7}}{911.06} \\ \eta &= 377 \Omega\end{aligned}\quad (4.19)$$

The Q factor can now be calculated using equation 4.20:

$$\begin{aligned}Q_{c2} &= \frac{\eta(kad)^3 b}{2\pi^2 R_s} \frac{1}{2l^2 a^3 b + 2bd^3 + l^2 a^3 d + ad^3} \\ &= \frac{377(9.11 \times 2.65 \times 10^{-3})^3 \times 1.27 \times 10^{-3}}{2\pi^2 \times 0.0818} \frac{1}{1.44257 \times 10^{-8}} \\ &= 2.653 \times 10^{-5} \times 69320657 \\ Q_{c2} &= 1839\end{aligned}\quad (4.20)$$

As stated above, since the cavity is filled with air, the Q factor of this dielectric, air, is negligible, since the Q factor is inversely proportional to and the resistance of air is very high. Hence the overall Q factor of the Gunn diode housing will be $Q = 1839$. Applying the above equations, the Q factor of the second harmonic waveguide is calculated to be $Q = 2154$. The Q factor of the circular backshort can be calculated in a slightly different way, as illustrated in equation 4.21:

$$\begin{aligned}Q_{c3} &= \frac{\eta(ka)^3 ad}{4P_{01}^2 R_s} \frac{1}{\left(\frac{ad}{2} + \frac{\beta a^2}{P_{11}}\right)^2} \\ &= \frac{377(9.11 \times 2.65 \times 10^{-3})^3 \times 2.65 \times 10^{-3}}{4 \times 1.841^2 \times 0.0818} \frac{1}{5.08 \times 10^{-6}} \\ &= 0.067319275 \times 196599.6 \\ Q_{c3} &= 13235\end{aligned}\quad (4.21)$$

Therefore the overall Q factor of the circular backshort will be 13235. Increasing the conductivity of the material will increase the Q factor further. Comparing the results of the three components:

$$Q_{\text{housing}} = 1839 \quad Q_{2\text{ndharmonic}} = 2154 \quad Q_{\text{backshort}} = 13235$$

The area for concern is the component with the lowest Q factor. The Gunn diode housing has the lowest Q factor of $Q = 1839$, This value is greater than the minimum desired value of $Q = 1000$, and this value can be improved by plating the walls with a better conductor such as gold or silver.

4.1.5 Summary

The design of the single device oscillator was modified since the interim report. The modification includes a new backshort. The power losses and quality factor of the oscillator have been calculated and found to be good; power loss was low and the quality factor was high. The manufacturing of the single device oscillator was completed by mid March and testing has begun, with the intention of using this test data for the development of the multiple device oscillator.

4.2 Radial line transformer

4.2.1 Introduction

The radial line transformer (RLT) is a crucial part of the circuitry inside the oscillator system. It has three functions: to provide a bias to the diode, to act as a filter and a resonator. Its most important role is to provide a DC bias to the Gunn diode. This could be achieved by applying a voltage to a simple metal pin and placing the pin on the diode, but if this method were used, much of the output RF energy would leak away along the pin. This possible signal leakage is the reason why the RLT fulfils the other two functions, so that the efficiency of the Gunn diode system is maximised. The RLT filter will reflect back into the cavity the useful energy at the first and second harmonic frequencies. The RLT resonates at the fundamental frequency of the system.

Figure 4.7 shows the RLT placed inside the RLT cavity. A hole, the RLT cavity, is drilled into the waveguide housing and the RLT sits inside it on top of the Gunn diode. Insulation tape is wrapped around the RLT filter circuit to prevent it from touching the wall of the waveguide housing (which is grounded) and resulting in a short circuit.

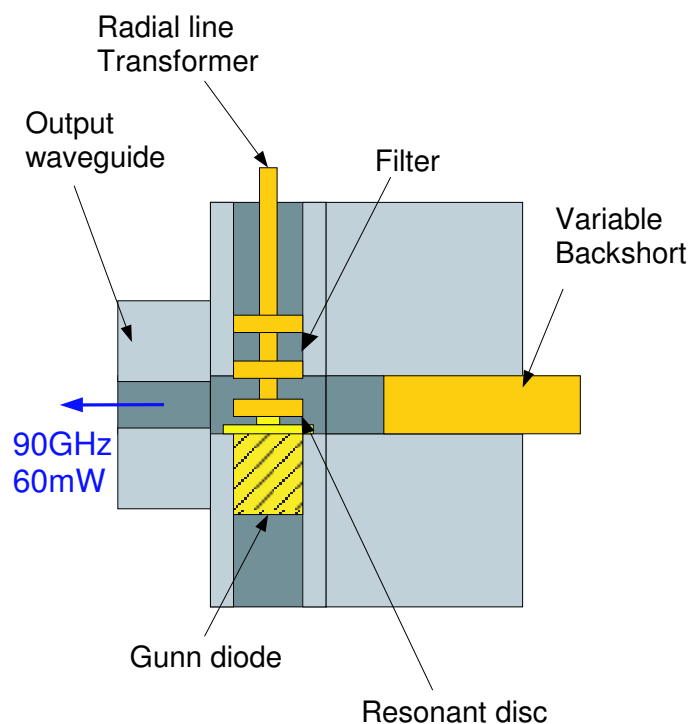


Figure 4.7: Radial line transformer in the waveguide cavity

The resonant disc is a disc that is positioned on the RLT between the filter and the Gunn diode. The resonant disc has a single purpose, to resonate at the fundamental frequency.

In order to attain the maximum efficiency, the structure of the RLT must be designed and each dimension determined. There are three ways to ascertain the dimensions: mathematical calculations, computer simulations, and physically building and testing the RLT. To use the method of physically building and testing the RLT, experience and a good practical knowledge of the RLT are required. The engineer will manufacture a standard RLT of mathematically calculated or known dimensions to match the frequency of operation, and then fine-tune the RLT by testing it in the circuit and altering the dimensions where necessary, usually with a fine chisel on a lathe. The project team has no working knowledge of the RLT, so this method would be otiose, therefore the other two methods shall be discussed.

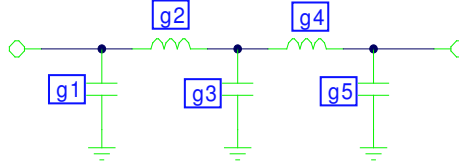


Figure 4.8: Filter circuit components

4.2.2 Filter circuit

The filter circuit comprises of a succession of inductors and capacitors; a low pass filter. The component equivalent of the filter can be seen in Figure 4.8.

The aim of the low pass filter circuit is to inject the maximum DC current into the Gunn diode whilst stopping any RF energy leaking out of the oscillator. The first step is to mathematically determine the values of inductors and capacitors. A book called *Microwave filters, impedance-matching networks, and coupling structures* (Matthai, Young & Jones 1980) was used to accomplish this.

Parameters such as the corner frequency and ripple were suggested in this book. The corner frequency is the point at which the filter starts to work and it is desirable that there is fast roll off at this point. Fast roll off means that as the frequency increases the amount of rejection increases rapidly. This is visible on a graph as the signal dropping sharply. The corner frequency was chosen as 30 GHz because with a fast roll off the rejection will be high at 43.5 GHz, the fundamental harmonic frequency. The amount of ripple chosen was -3 dB, this is a large amount of ripple, and was chosen because it will not affect the DC signal and it produces a faster roll off.

To find the relevant capacitances and inductances, tables can be used (Matthai et al. 1980, p101) to provide de-normalised values at 1Ω and 1 Hz, but these values need to be converted to represent the design. For the chosen filter structure, $n = 5$, where n is the number of capacitors and inductors in the RLT structure: three capacitors and two inductors are used in the design, and the de-normalised values are:

$$g_1 = 3.4389 \quad g_2 = 0.7483 \quad g_3 = 4.3471 \quad g_4 = 0.5920 \quad g_5 = 5.8095$$

For the capacitances g_1 , g_3 and g_5 , equation 4.22 is applied.

$$C = \frac{R'_0 \omega'_1}{R_0 \omega_1} g_1 \quad (4.22)$$

Where:

$$\begin{aligned} R'_0 &= 1 \\ R_0 &= 50 \Omega \\ f'_1 &= 30 \text{ GHz} \end{aligned}$$

$$\text{For } g_1, C = \frac{1}{50} \frac{1}{2\pi \times 30 \times 10^9} \times 3.4389 = 0.365 \text{ pF} \quad (4.23)$$

For the inductances, g_2 and g_4 , equation 4.24 is applied:

$$L = \frac{R_o \omega'_1}{R'_o \omega_1} g_2 \quad (4.24)$$

$$\text{For } g_2, L = 50 \frac{1}{2\pi \times 30 \times 10^9} \times 0.7483 = 0.1985 \text{ nH} \quad (4.25)$$

Once the filter circuit component values are known they have to be converted into the dimensions of coaxial line. Coaxial theory is used and equations 4.26 and 4.27 are used for the capacitors and inductors respectively (Matthai et al. 1980).

$$d = \frac{C}{\frac{2\pi\epsilon_0}{\ln \frac{b}{a}}} \quad (4.26)$$

$$d = \frac{L}{\frac{\mu_0}{2\pi} \ln \frac{b}{a}} \quad (4.27)$$

Figure 4.9 shows the dimensions of a , b and d .

In order to find a value for d , fixed dimensions were chosen for a and b (Matthai et al. 1980). For the capacitor, the gap between a and b is required to be as small as possible because this makes a higher value capacitor. Similarly, for the inductor, the gap between a and b should be as large as possible to make a higher value inductor. The value for a_C was chosen to be 2.8 mm and b_C was 3 mm for the capacitors and for the inductors a_L was 1 mm and b_L 3 mm.

The dimensions yielded can be seen in table 4.1.

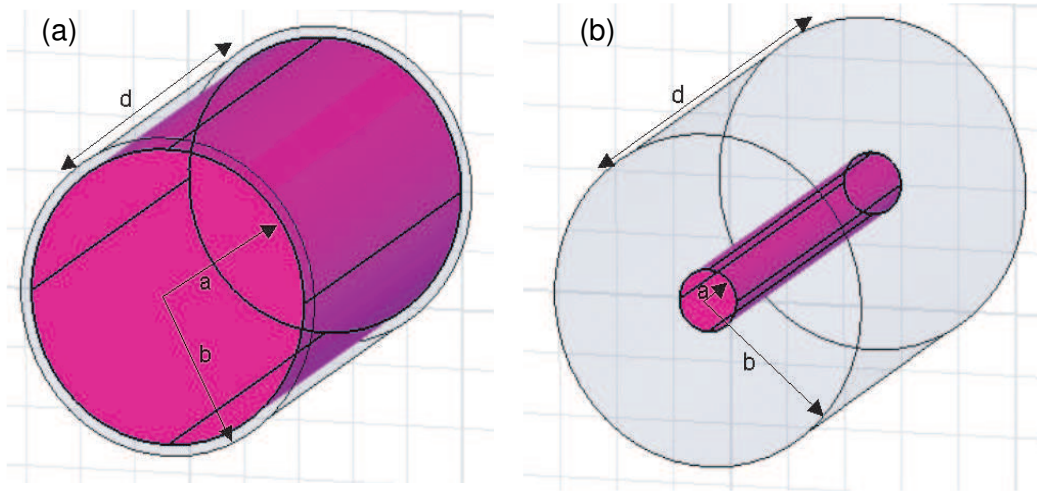


Figure 4.9: Coaxial line dimensions: (a) Capacitor, (b) Inductor

Table 4.1: Radial line transformer filter circuit dimensions

Component	a (mm)	b (mm)	d (mm)
C_1	2.8	3.0	0.45
C_2	2.8	3.0	0.57
C_3	2.8	3.0	0.76
L_1	1.0	3.0	0.90
L_2	1.0	3.0	0.70

4.2.3 Advanced Design System (ADS)

Once the dimensions of the filter have been calculated using mathematical theory, the values are entered into a simulation package called Advanced Design System (ADS). ADS contains, among other things, a circuit simulator intended primarily for the designs of RF/microwave frequency systems.

First, the capacitor and inductor component values, calculated using theory, are entered into ADS. This is done to verify that the circuit will respond in the desired way and that no mistakes were made during the calculation stage. Figure 4.10 shows a screenshot from ADS, of the components with each end of the configuration terminated with $50\ \Omega$. The S-parameters were set up so that the results could be seen across a range of 1–100 GHz, which includes the frequencies of interest; the fundamental (43.5 GHz) and second

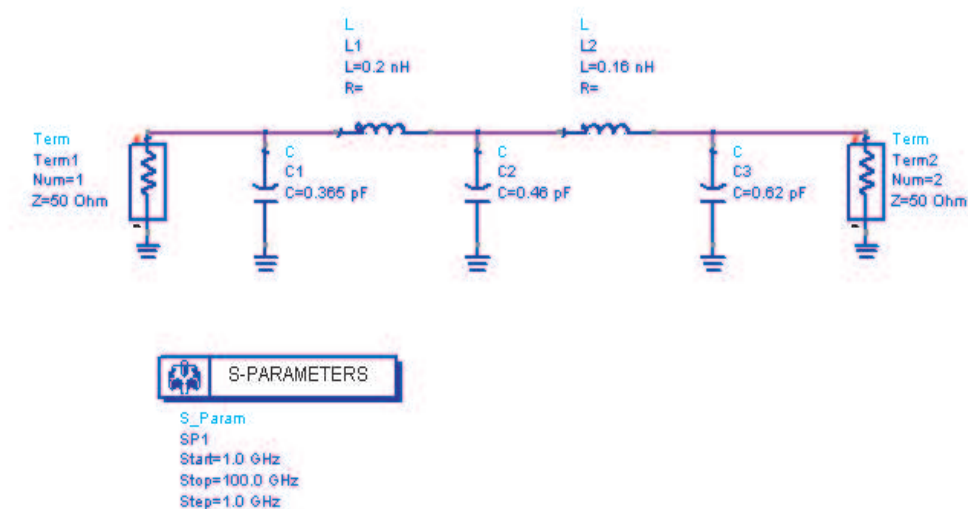


Figure 4.10: Screenshot of components from ADS

harmonic (87 GHz). The circuit was simulated and the results can be seen in Figure 4.11.

On the graph the ripple can be seen at the low frequencies and a sharp roll off occurs at 30 GHz, which matches the design specifications set out at the start. It is desired that there should be at least -20dB of rejection at the fundamental and second harmonic. This is equal to the power being attenuated by 99% or greater. At the fundamental frequency the rejection is about -35 dB, which is better than our desired figure. At the second harmonic the rejection is even better, at -70 dB. The simulation results match the theory and verify that the RLT design made using the mathematical calculations is effective as a filter. The next step is to validate the coaxial dimensions that have been calculated.

The components are entered into ADS as lengths of coaxial line which are terminated with 50Ω . Figure 4.12 is a screenshot from ADS showing the coaxial lines joined together.

The filter was simulated in the same way as before over the frequency range 1–100 GHz. Figure 4.13 is the plot of these results.

The graph shows the ripple at the top, at low frequencies, and the roll off begins just before 30 GHz. At the fundamental frequency the rejection is about -35 dB, which is the same as for the component filter. At the second harmonic the rejection is -60 dB, this is not as good as for the component

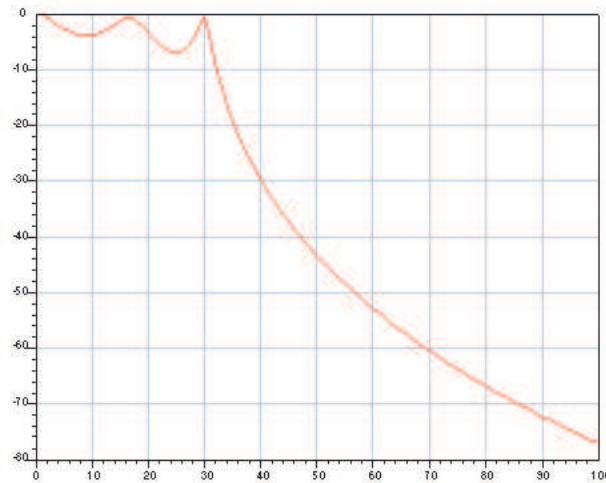


Figure 4.11: S-parameter plot of filter circuit with components from ADS

filter but is still a good value because only a minute proportion of the energy is leaking away, just $10^{-4}\%$.

ADS has been successfully used to validate the design for the filter and the next step is to enter the design into another simulation package called HFSS.

4.2.4 High Frequency Structure Simulator

High Frequency Structure Simulator (HFSS) is a software package which allows the user to enter a design as a three-dimensional object and define the boundaries and excitations. HFSS uses Maxwell's equations to solve the problems posed to it; to determine the behaviour of the electric field of a 3D object at a certain frequency. To obtain results, the frequency or frequency range and mesh conditions must be specified. It is not possible for HFSS to determine the electric field by solving Maxwell's equations across the whole object, particularly not if the object is a complex shape.

To overcome this, HFSS generates a mesh of tetrahedrons across the surfaces of the object and then calculates the electric field in the tetrahedrons using a second order polynomial containing unknown coefficients. The matrix is then solved to determine the values for the polynomial coefficients resulting in an approximation of the electric field across the whole object.

The low pass filter design was entered into HFSS as a succession of cylinders whose dimensions have been calculated and stated in table 4.1. The cylinders

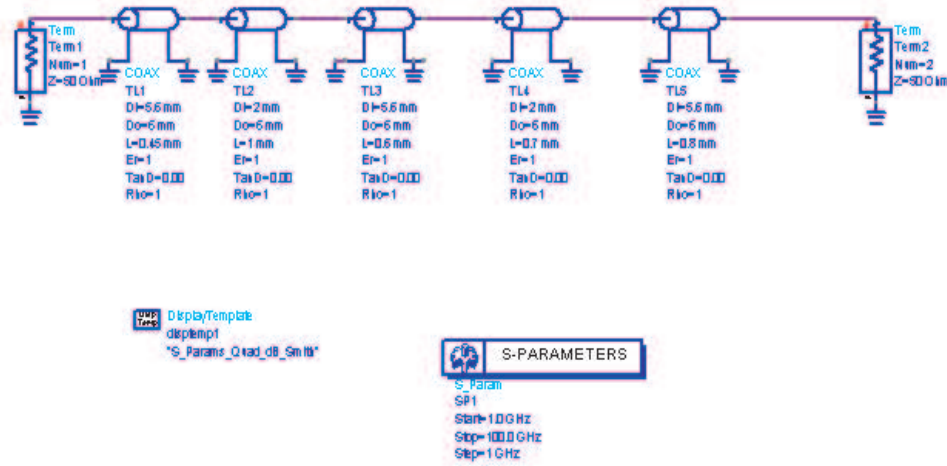


Figure 4.12: Screenshot of coaxial lines from ADS

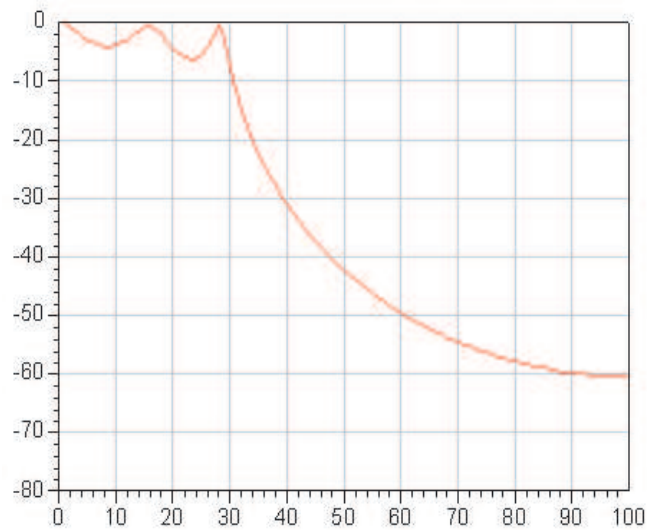


Figure 4.13: S-parameter plot of filter circuit with coaxial line from ADS

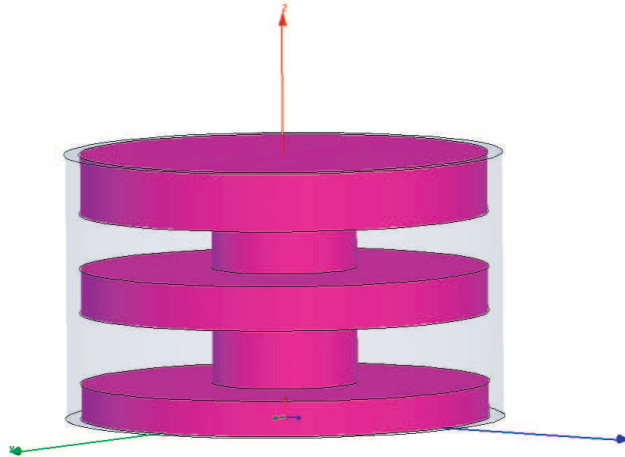


Figure 4.14: Screenshot of filter design from HFSS

are defined as perfect conductors. Figure 4.14 shows the 3D representation of the filter.

The transparent outer cylinder around the filter is the waveguide housing, the RLT is sat inside the RLT cavity which is defined as air-filled and the waveguide edge is defined as a perfect electrical boundary (E boundary). Two ports were created, port 1 at the top and port 2 at the bottom of the filter. The ports are where the excitation can be measured. The top of the structure is the top of the waveguide housing and the bottom of the structure is the waveguide cavity. A mesh was created along the inside of the waveguide housing and outside of the RLT structure and the simulation was run. Figure 4.15 shows the results of this simulation.

This S-parameter plot shows that the desired response is not achieved from the filter. Roll off begins immediately, resulting in the rejection decreasing from 0 GHz. The rejection reaches a minimum of -64 dB at 41 GHz, and then rises back to no rejection before falling again. At the fundamental frequency the rejection is -60 dB, which is even better than the result from ADS, but at the second harmonic frequency the rejection is only -5 dB. This is a very poor result, the desired rejection is at least -20 dB. The problem occurs because the rejection falls initially but then rises and falls again, whereas the response in ADS was; once the rejection started increasing, it continued to do so as the frequency increased.

To solve the problem that the rejection was not large enough at the second harmonic, the dimensions of the components on the RLT were changed to a

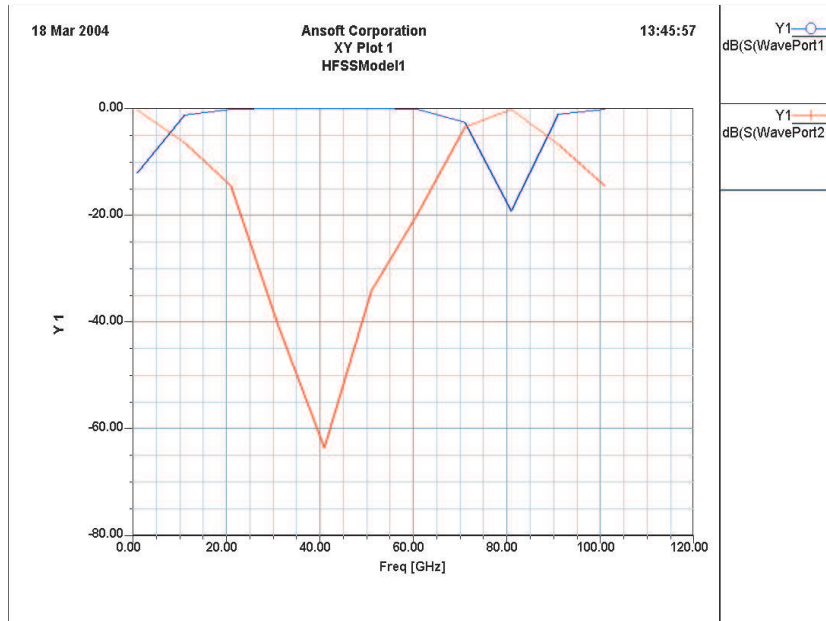


Figure 4.15: S-parameter plot from HFSS of original design

number of different magnitudes. It was hoped that component dimensions would be found that would cause the graph to be shifted to the left so that the rejection would be sufficiently low at the second harmonic. It was decided that the radius of the RLT cavity would be reduced from 3 mm to 2 mm, and that the gap between the waveguide housing and the capacitor would remain at 0.2 mm so the radius of the capacitors was reduced to $r_C = 1.8$ mm and the radius of the inductors remained at $r_L = 1.0$ mm. Shortening the the radius of the RLT discs will result in the cut-off frequency occurring at a slightly higher frequency than calculated in section 4.1.2.2.

These changes were made to the design and then it was simulated. Figure 4.16 shows the results of this simulation.

The expected result was that the previous graph would be shifted to the left but the actual result is similar to the graphs from ADS. There is a small amount of ripple at the start and the roll off begins at around 30 GHz. At the fundamental frequency the rejection is -15 dB, which is less than the desired value of -20 dB but is still acceptable. At the second harmonic the rejection is -40 dB, which is a good value.

The RLT structure up to this point is comprised of three capacitors and two inductors, so $n = 5$. Another way of designing the filter is to use two

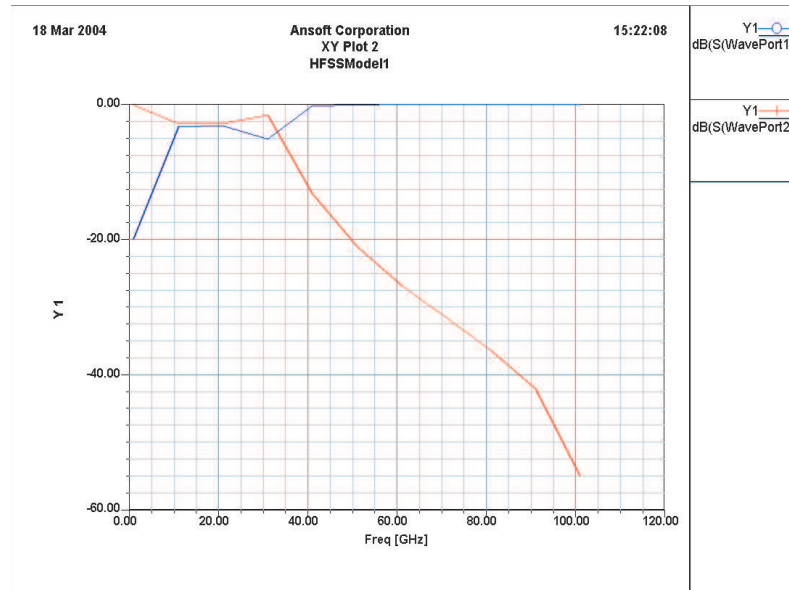


Figure 4.16: S-parameter plot from HFSS of reduced radius design

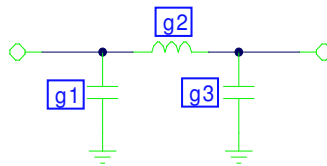


Figure 4.17: New filter circuit components

capacitors instead of three. An investigation into this filter was completed so that the two capacitor design could be compared with the three capacitor design.

4.2.5 Filter with two capacitors

In order to design a low pass filter with only two capacitors, the same steps were taken as with the three capacitor filter. Figure 4.17 shows the component equivalent of the new filter.

The table of de-normalised values for the capacitors and inductors was used (Matthai et al. 1980, p101), and the de-normalised values were converted

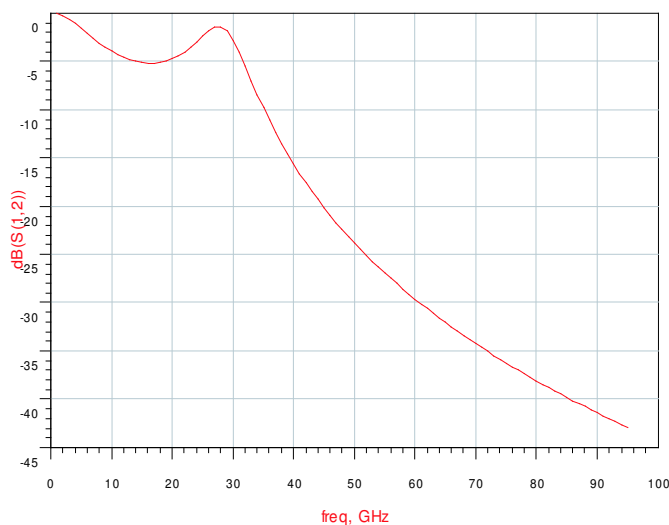


Figure 4.18: S-parameter plot: two capacitor filter with components (ADS)

to component values. The component values were then entered into ADS. Figure 4.18 shows the S-parameter plot of the results, and figure 4.19 is the S-parameter plot for the components converted into coaxial line.

It is clear that, by comparing these graphs (figures 4.18 and 4.19) with the other ADS graphs (figures 4.11 and 4.13), the three capacitor low pass filter is more effective at reflecting the RF energy back into the waveguide cavity. The three capacitor filter has greater rejection than the two capacitor filter. At the fundamental frequency, the two capacitor filter has a rejection of -16 dB, whereas the three capacitor filter had -32 dB of rejection. At the second harmonic the two capacitor filter only has -35 dB of rejection, whereas the three capacitor filter had -60 dB of rejection. So, it can be seen that the three capacitor filter has a rejection that is approximately ten times as good as the two capacitor filter according to the ADS simulations. For this reason it was decided that a three capacitor filter would be manufactured.

4.2.6 Resonant disc

The resonant disc is positioned between the RLT filter and Gunn diode. The purpose of the disc is to resonate at the fundamental harmonic frequency. The disc increases the stability of the oscillations if it is resonating at the same frequency as the Gunn diode. If the disc is resonating at a different frequency from the diode the stability of the oscillation is reduced and some

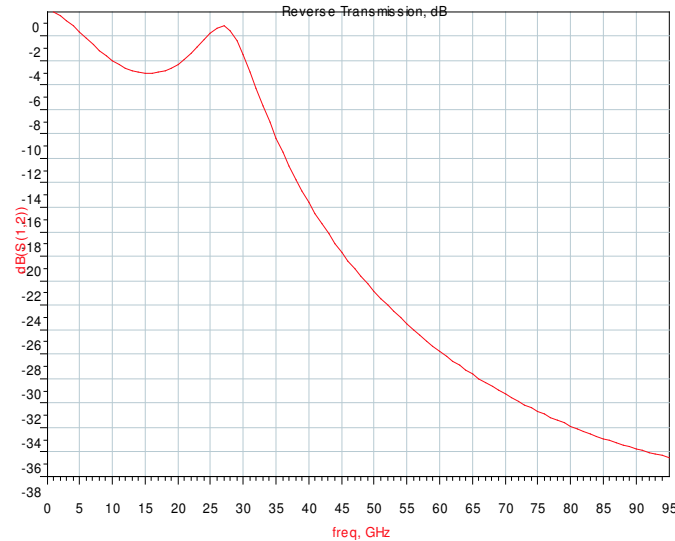


Figure 4.19: S-parameter plot: two capacitor filter with coax line (ADS)

of the RF signal from the diode is absorbed to maintain the disc resonance, the result is the output signal is reduced.

A trial and error approach was adopted to design the resonant disc. The resonant disc is difficult to design and the normal design process is to manufacture a disc of ideal diameter that will resonate at the desired frequency, but the disc always needs fine tuning. This fine tuning is unavoidable because there are always small errors of about ± 0.02 mm in the size of the components due to the manufacturing tolerances.

The aim of the simulation is to determine the ideal disc diameter, so that the disc will resonate at the fundamental frequency if all the component dimensions are exact.

The resonant disc is simulated only in HFSS because its physical dimensions are the only values of interest. Because of the symmetry of the disc and energy waves in the system, the simulation comprises of just half of the disc inside the waveguide. Using half of the disc reduces simulation time since the simulation computation is halved. Underneath the disc a lumped port was set up; this internal port is to simulate the Gunn diode. Figure 4.20 shows the HFSS design of the disc.

An S-parameter plot was set up to analyse the phase change at different frequencies. There was a phase change between 35 and 36 GHz so the plot

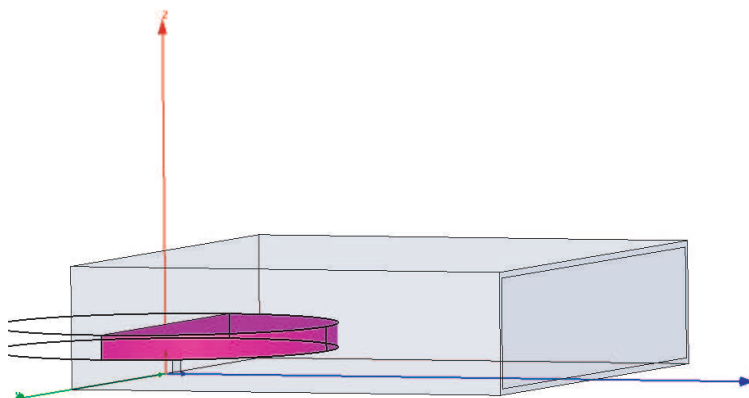


Figure 4.20: Half a resonant disc in the waveguide

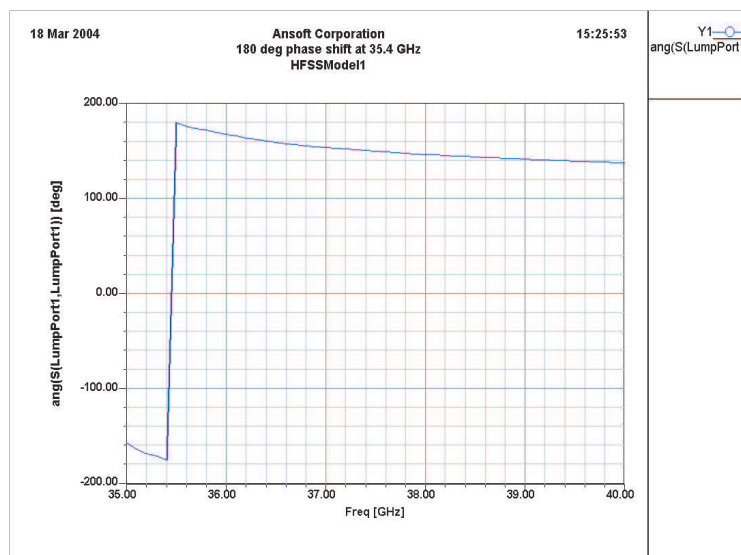


Figure 4.21: Frequency against angle for half a resonant disc

was run across a smaller range so that this point could be enlarged and examined. Figure 4.21 shows the S-parameter plot between 35 and 40 GHz.

There is a phase change from -180° to 180° at 35.4 GHz. It is believed that this phase change is a result of resonance at this frequency. To shift the phase right, towards 43.5 GHz the disc diameter was reduced and the simulation was run again. Figure 4.22 shows the result of this simulation.

This plot shows that a similar phase change now occurs at 37 GHz, suggesting

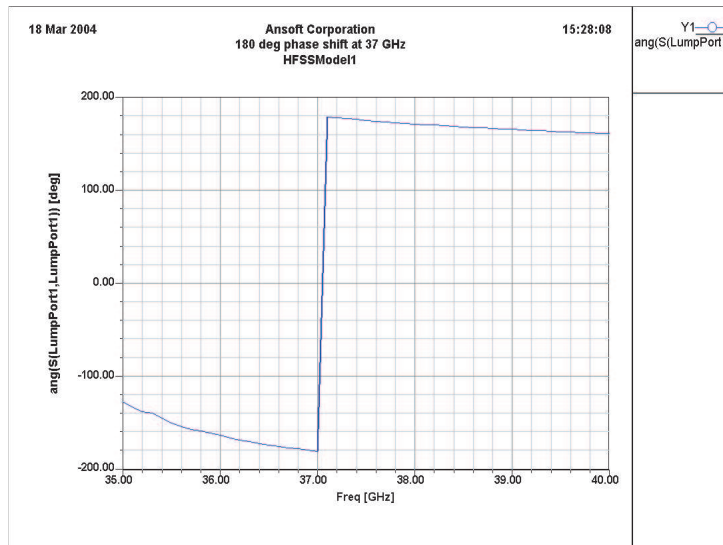


Figure 4.22: Frequency against angle for smaller half resonant disc

that by reducing the diameter of the disc the resonance moves to a higher frequency. Several simulations were run to investigate this and for the resonance to occur at 43.5 GHz the disc diameter must be 1.9 mm. Figure 4.23 shows the S-parameter plot of this simulation.

Philip Norton of e2v Technologies is an expert in the area of Gunn diodes and particularly the RLT and resonant disc. Philip determines the value of the disc diameter by conducting practical tests. Tests he conducted suggested that the disc's diameter should be 2.4 mm to begin with, then the RLT is tested in the circuit and the disc's operation is optimised by removing 20 μm at a time on a lathe. The disc diameter, however, should not go below 2.1 mm as this is a typical starting point for an oscillator with a second harmonic frequency of about 94 GHz.

This difference led to the decision that the simulation should be modified to involve the entire disc enabling further observation of the disc and its behaviour dependant upon its diameter. Figure 4.24 shows the full disc in the waveguide, the lumped port is highlighted under the centre of the disc. The outer cylinder seen on the screenshot is a meshing area around the disc. The results of this simulation can be seen in Figure 4.25.

On this graph there are a number of phase changes at the higher frequencies suggesting that resonances occur at a number of high frequencies. Up to this point, the results have only considered one electric field mode, to analyse the

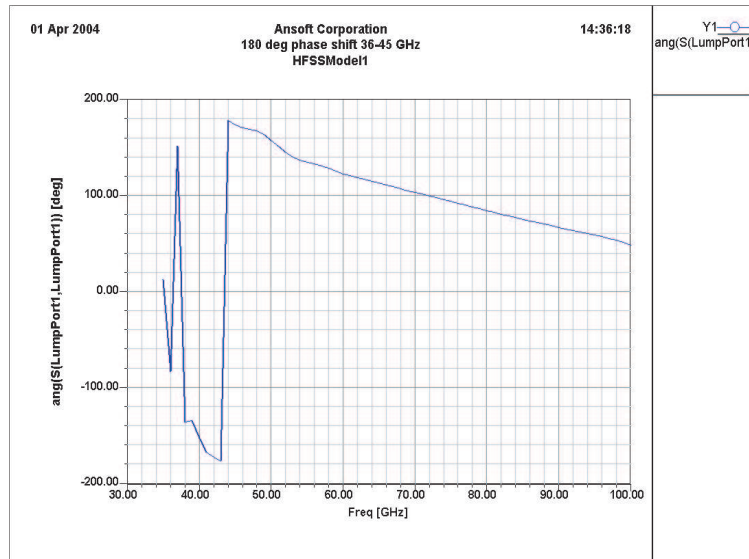


Figure 4.23: Frequency against angle for half resonant disc at 1.9mm

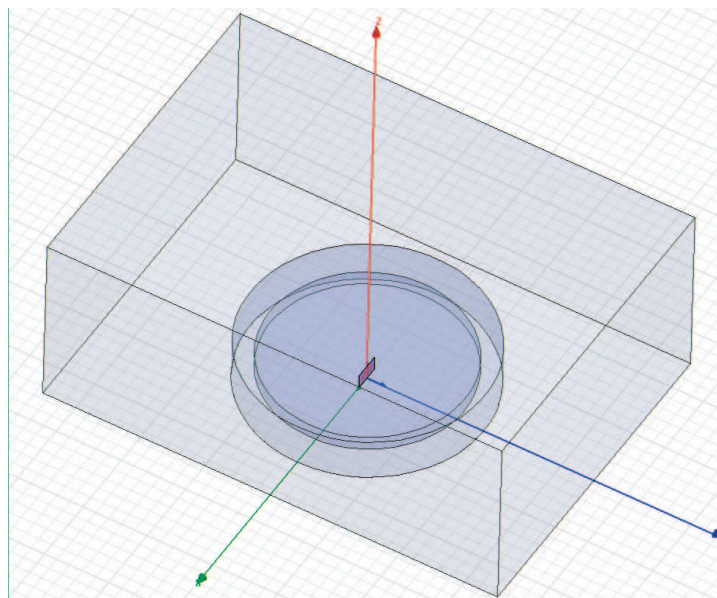


Figure 4.24: Full resonant disc in the waveguide

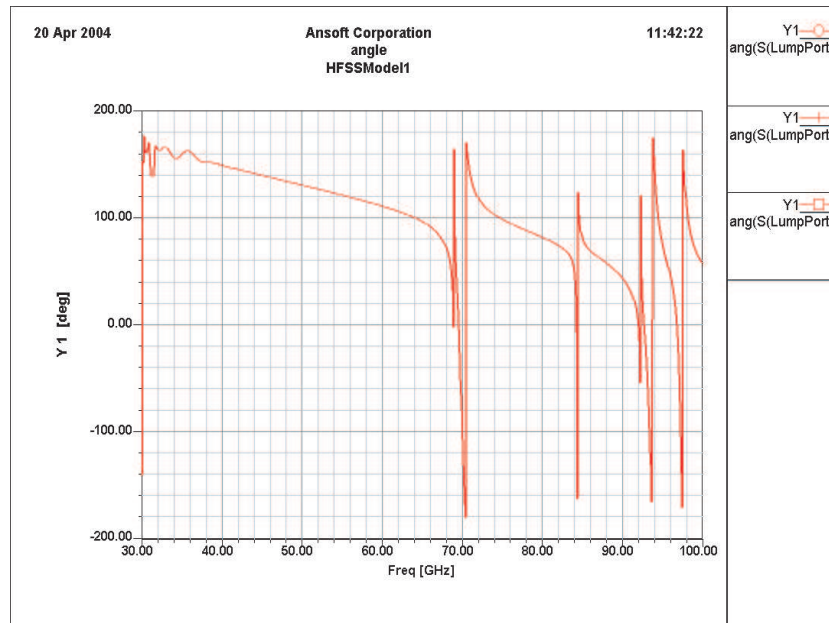


Figure 4.25: Frequency against angle for full resonant disc

numerous resonances the analysis was changed to include mode 1 and mode 2. Figure 4.26 illustrates the two modes. The modes are illustrated as the two arrows, one in the centre and one offset from the centre, on the shaded face. Analysing the additional mode means that the simulation can take up to an hour to run, which is much longer than earlier simulations, but it was hoped the more complex model would yield better results. The simulation was run and the plot set up to display the magnitude of the signal at port1 in dB. Figure 4.27 shows this plot.

The graph shows that there is a spike at around 81 GHz due to the resonance of the disc. By reducing the diameter of the disc this spike can be moved to the right on the graph and the resonance occurs at 87 GHz when the disc diameter is 2.6 mm.

Because of the different results gained by the three simulation methods: the half disc simulation, full disc simulation and full disc simulation analysing two modes, it has been decided that the simulation results are non-conclusive. So, we have decided that we will take advantage of e2v's knowledge and use a disc whose diameter has been calculated by the manufacturing and testing process. This disc diameter will be used since it has been verified that the disc will resonate at the desired frequencies.

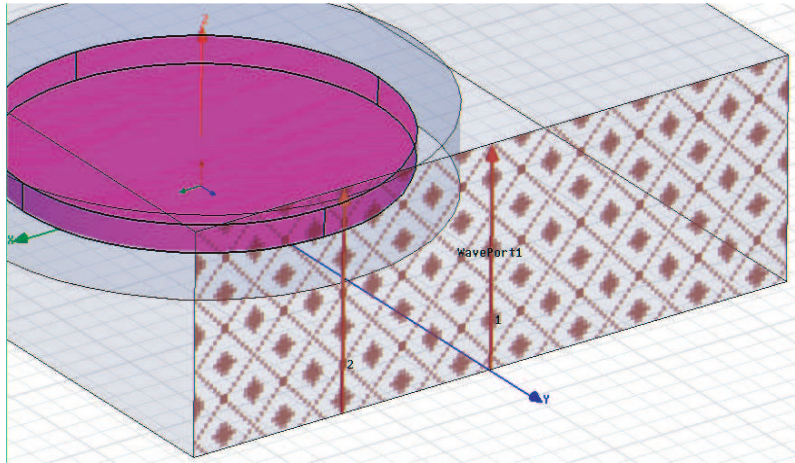


Figure 4.26: The two modes on the wave port

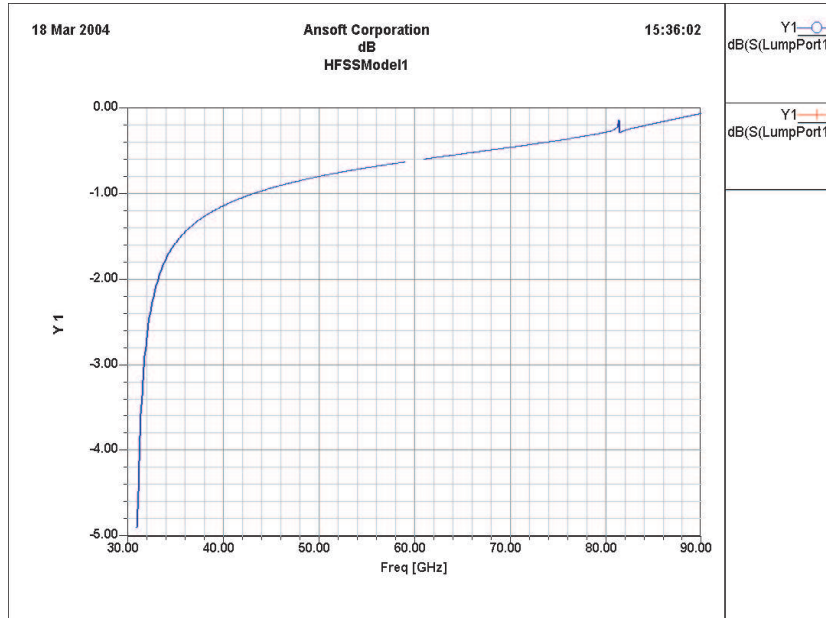


Figure 4.27: Magnitude plot for wave ports with two modes

It has been concluded that the current simulation model is insufficient to accurately model the system. For this reason, the lumped port was investigated because this is a crucial part of the model as it represents the Gunn diode. By changing the dimensions of the lumped port the system results changed dramatically, which led to the conclusion that a better model of the Gunn diode was needed.

4.2.7 Gunn diode model

After discussions with e2v Technologies' engineer Keith Newsome it was discovered that e2v use a more accurate Gunn diode model. The model is defined as a GaAs substrate with a rectangular lumped port across the top, on top of this there is a Maltese cross arrangement. The reason for using this set up is that it physically and mathematically models the Gunn diode far more accurately than a simple lumped port and as the results have proven, the lumped port can affect the results dramatically. A planar Gunn diode oscillator designed, manufactured and sold by e2v has been simulated using the more accurate diode model and their results conclude that the model functions as desired and generates the expected results.

This led to the conclusion that when simulating a Gunn diode oscillator, great care must be given to the Gunn diode model. The model must represent the diode as accurately as possible in order to achieve meaningful results. The next aim for the simulation is to use this accurate Gunn diode model to investigate the effects of the resonant disc sufficiently and determine its diameter. The improved diode model will help the simulation investigations of the project a great deal, but there is the need for a simulation package to be created which can model the internal and external effects of a Gunn diode to allow the diode to be investigated and understood further. Currently no such model is available and the only solution is to use the e2v lumped port model.

4.2.8 Future work

The simulation work is still ongoing, and the future work is the tasks for the team to do before the project completion. The first objective of the future work is to determine the exact dimensions of the RLT using HFSS and to model it to prove it provides the correct bias, with a working filter and resonator. In order to achieve this the Gunn diode model will have to be improved so that the results are more representative of real life. The filter

circuit has been proven to work using theory and simulation packages but the resonant disc still needs more work. The main focus of the simulation will be to create a better Gunn diode model and to use this model to investigate the resonant disc and determine its dimensions.

Once the RLT dimensions have been determined using simulation, the RLT will be manufactured. The RLT defined using mathematical calculations, as described in section 4.2.2, and the RLT designed by Philip Norton of e2v, made using informed guesses, practical testing and tuning, will also be manufactured and the three RLTs will be compared with each other. Each of the three methods will yield different designs that can be tested in the Gunn diode oscillator designed by the team proving which is the best method to design and determine the dimensions of a RLT.

4.2.9 Summary

The RLT dimensions have been determined by a combination of three methods; mathematical calculation, simulation and, manufacturing and testing. The dimensions of the filter section of the RLT have been fully defined but further work must be carried out to determine the dimensions of the resonant disc. Work is also being carried out to produce a more accurate model of the Gunn diode than the lumped port that has been used up to this point. When the resonant disc dimensions have been determined the RLT will be re-simulated with the new model of the Gunn diode. A decision has been made to manufacture three different RLTs and compare their performances in the oscillators.

4.3 Testing

4.3.1 Introduction

This section looks at the ways in which the Gunn diode oscillator is set up to produce a required frequency at maximum power output and the testing and verification that was applied to the system. It shows that this is a complex task with many variables which must be taken into consideration.

The testing of the device was undertaken in two stages: the first was at the e2v Technologies labs in Lincoln and second was in the labs at UMIST. Ideally, we would have used the results of this testing in the design of the multiple device oscillator; for example, the optimal backshort cavity length

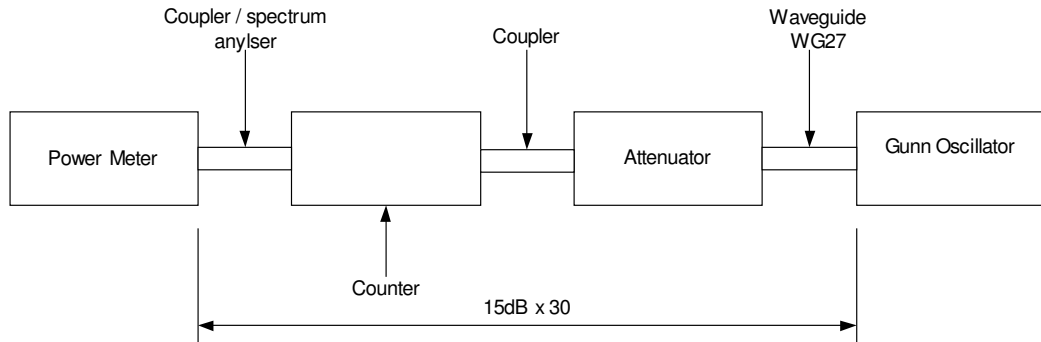


Figure 4.28: Test setup at e2v Technologies

is double a multiple of the optimal distance between diodes in a multiple diode oscillator. However, due to problems with the device manufacture as described in section 6.1, the designs for the multiple device oscillator had to be submitted before testing the single device oscillator had been completed.

4.3.2 Device set up and e2v test rig

The test rig used at e2v Technologies consists of five main components interconnected through waveguide extensions. The first component is the Gunn diode oscillator. The output of the oscillator is fed directly into a rotary vein attenuator, the second component. The output of the attenuator is fed into the third component, a digital counter to measure frequency, to the fourth component an external mixer of a spectrum analyser and then to the fifth and final component, a power meter. The attenuator is set to give a nominal attenuation of 15 dB between the oscillator and the power meter. A block diagram of the set up is shown in figure 4.28.

4.3.2.1 Test method

The tests which are carried out and detailed below are tests to observe the power output, frequency of oscillation and the current drawn by the oscillator when the length of the backshort and the applied bias voltage are varied. The voltage is supplied and controlled by a variable, linear bench power supply. The backshort length is set using a digital vernier depth gauge. The bias voltage and current are measured with standard bench meters.

e2v carried out tests to measure the magnitude of the output power as the voltage and backshort length is varied. The bias voltage is varied from 4.5

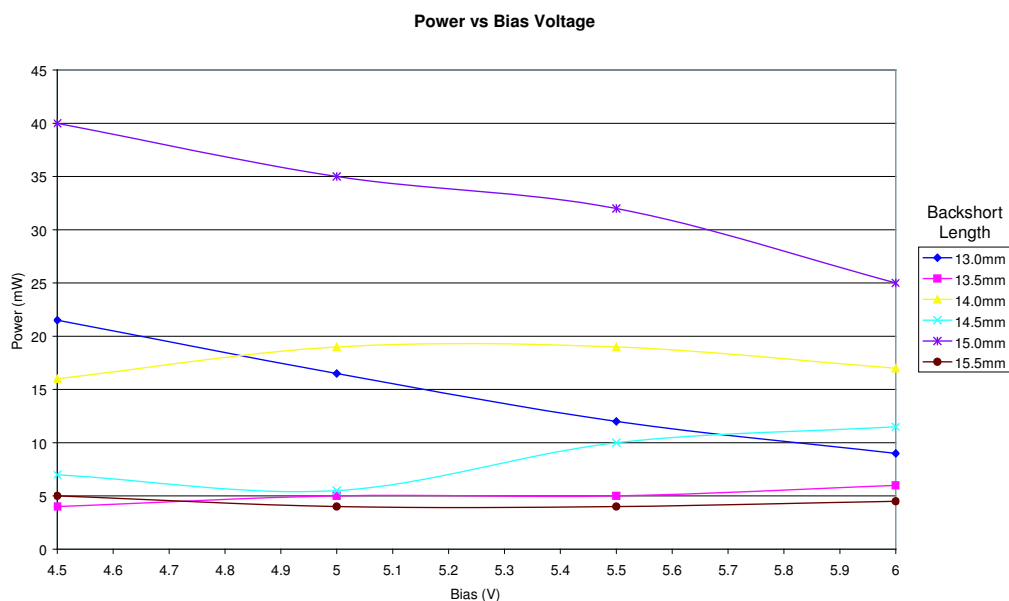


Figure 4.29: Graphs from e2v testing (1/2)

to 6.0 V in steps of 0.5 V for each backshort length, which is varied between 13.0 and 15.5 mm in 0.5 mm intervals. The results for each test are shown in appendix A.8. Graphs of each test are shown in figure 4.29.

4.3.2.2 Observations

It can be seen from the results tables in appendix A.8 that the current drawn from the supply varies very little with the backshort length and applied bias voltage. The maximum variation measured is under 10 mA. The frequency of oscillation also varies very little. The maximum power obtained from these coarse tests is 40 mW.

4.3.3 UMIST test rig

The test rig used at UMIST is a simpler version of that used at e2v. Instead of having a separate power meter and counter, a spectrum analyser is used to measure both the power and frequency. The test set-up is based upon the equipment used for testing the e2v oscillator as described in section 3.7 of the interim report. However, instead of a fixed air gap between the oscillator

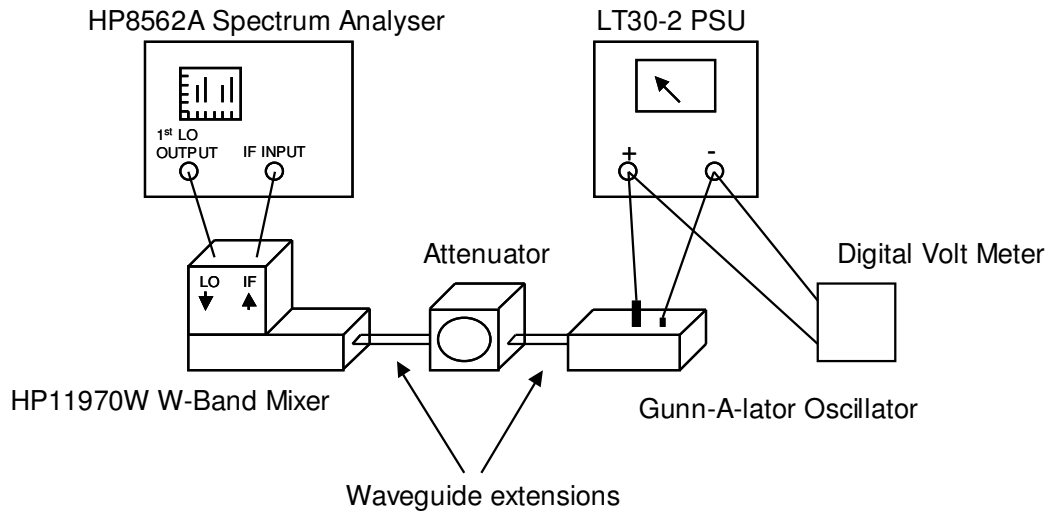


Figure 4.30: Test setup at UMIST

and the mixer, an attenuator has been used to accurately set the attenuation level. A block diagram of the set-up is shown in figure 4.30.

4.3.3.1 Test method

The oscillator is set up following the procedure in section 3.7.1.3 of the interim report. The final step, step 8 in the interim report, is replaced by the following procedure:

8. Using two waveguide extensions connect the oscillator to the attenuator and the attenuator to the mixer using the captive screws supplied. It is important at this stage not to tighten up the flanges as this is difficult to do by sight and excess leakage may occur as a result. The attenuation value should be set to 25 dB to ensure that excess power levels will not damage the mixer. When the spectrum analyser is set up to read the power output from the working oscillator the flanges should be tightened. Each flange should be tightened in turn by a small amount and the process repeated whilst carefully watching the power reading. As the flanges are tightened the power should increase as the leakages are reduced. If the flanges are not exactly parallel then a decrease in power will be observed.

The spectrum analyser is set up following the procedure in section 3.7.1.4 of the interim report with the addition of the following steps:

7. Select “Amplitude” from the analyser front panel followed by the “Linear” soft key.
8. Select “Amplitude” from the analyser front panel followed by the “more” soft key and the “Ref LVL Offset” soft key. Type “25” in to the number pad and press the “dB” button on the Data Panel. This is the attenuation level as set and ensures that the spectrum analyser scales its display accordingly.
9. Select “Amplitude” from the analyser front panel followed by the “more” soft key, the “units” soft key and the “Watts” soft key. This allows the power output to be read in milliwatts.
10. Select “Amplitude” from the analyser front panel followed by the “Ref LVL” soft key. Type “50” in to the number pad and press the “mW” button on the Data Panel. This sets the display to show a maximum of 50mW output
11. Select “Frequency” from the front panel followed by the “Center Freq” soft key. Type “85” in to the number pad followed by pressing the “GHz” button on the data panel.
12. Select “Span” from the front panel followed by the “Span width” soft key. Type “5” in to the number pad followed and press the “GHz” button on the data panel.
13. When the oscillator is on, two peaks should show on the screen. One real peak at the oscillation frequency and one image. The desired peaks may be selected by pressing the “Peak search” key of the front panel and the “next peak” soft key. When a peak is selected with the cursor the “signal identity” function of the analyser is used. Select Mixer→“Ext” from the front panel. Then select the “Signal Ident” soft key followed by the “Sig ID at mkr” soft key. After a few moments the analyser will display the frequency of the detected oscillation. If the peak selected is an image the analyser will also state this.
14. When varying the oscillation frequency it is useful to have the spectrum analyser track the signal. Press “Peak search” from the front panel followed by the “Sig trk on” soft key.
15. When taking a reading it can be useful to freeze the display. This can be done by pressing the “Sweep” key on the front panel, followed by the “single” soft key.

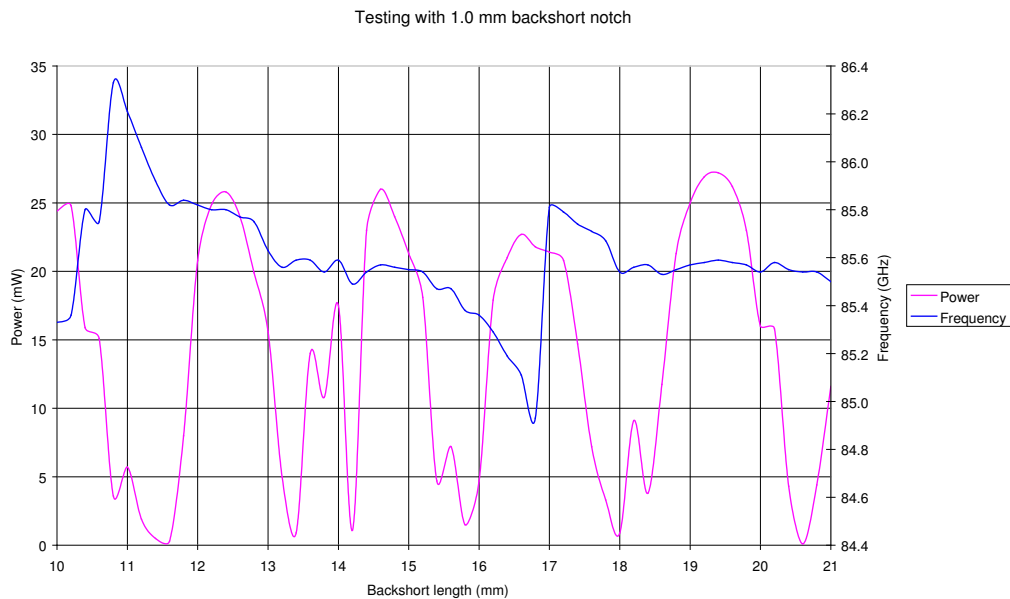


Figure 4.31: Results of testing with a 1.0 mm backshort notch

Test 1: To observe the effect of varying the length of the backshort, on power and frequency. A backshort with a 1 mm second harmonic notch is used.

1. Set the bias voltage to be a constant 4.5 V. Switch on the supply.
2. Set the length of the backshort to 21.0 mm using a digital vernier depth gauge.
3. Measure the frequency of oscillation and the power output by selecting the relevant peak on the spectrum analyser as described above.
4. Keeping the bias voltage as 4.5 V, reduce the length of the backshort by 0.2 mm
5. Repeat steps 3 and 4 until the backshort is of length 13.0 mm. Due to the geometry of the oscillator it is difficult to use backshort lengths outside of this region.
6. The results of this are shown in appendix A.8. A graph of the results is shown in figure 4.31.

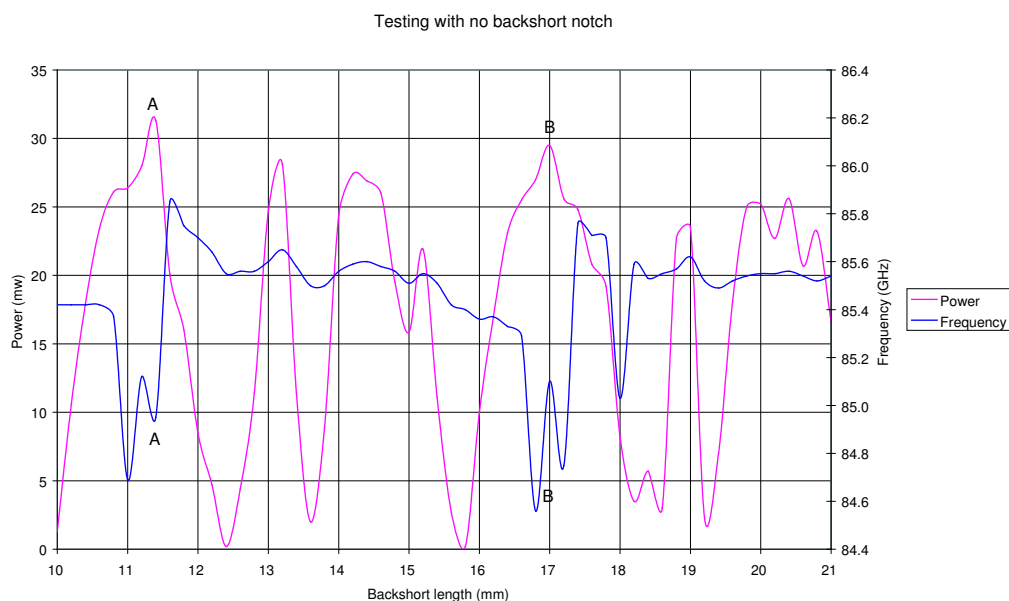


Figure 4.32: Results of testing with no backshort notch

Test 2: To observe the effect of varying the length of the backshort, on power and frequency. A backshort with no second harmonic notch is used. This is the same procedure as for Test 1 above. The results of this are shown in appendix A.8. A graph of the results is shown in figure 4.32.

Test 3: To observe the effect of varying the applied bias voltage, on power and frequency. The backshort length is fixed.

1. Set the bias voltage to be 4.5 V. Switch on the supply.
2. Vary the length of the backshort until the highest power output is obtained. Fix the backshort at this length.
3. Reduce the applied bias voltage to 3.5 V
4. Record the power output and frequency using the methods discussed.
5. Increase the bias potential by 0.2 V and repeat steps 4 and 5 until a maximum bias of 6.1 V is read.
6. The results of this are shown in appendix A.8. A graph of the results is shown in figure 4.33.

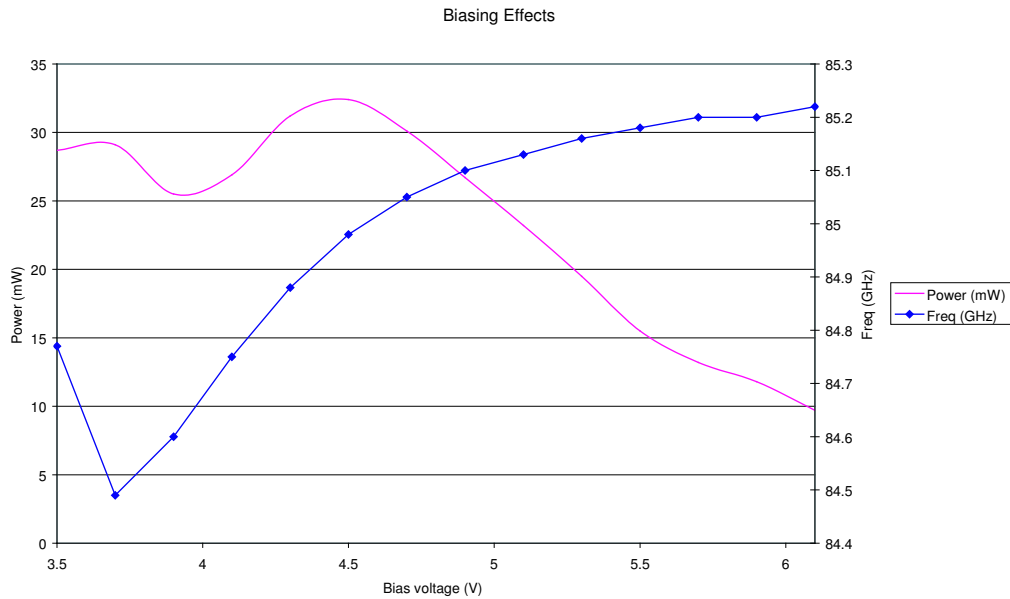


Figure 4.33: Biasing effects

4.3.4 Test result analysis

In line with the observations from testing e2v's commercial single device oscillator, the output of the oscillator is highly dependant on the system conditions, such as the cavity length and shape and the bias voltage.

Through the coarse testing of our device at e2v Technologies, we were able to obtain an approximate set up for the best power output of 50 mW at 85.05 GHz. With exactly the same setup using UMIST's test equipment, we observed only 24.3 mW, even after cleaning all waveguide extensions.

On investigation, it was discovered that the spectrum analyser, mixer and attenuator had not been calibrated. Calibration will be performed after Easter, but this does not leave enough time to re-take these results and comment on the new findings. The equipment should, however, be calibrated in time for testing the multiple device oscillator.

If we assume that there is a total of 3 dB uncalibrated attenuation in our equipment, as suggested by the difference in readings of the device under the same test conditions measured at e2v then at UMIST, we can show that the more in-depth testing at UMIST has revealed conditions leading to an even greater RF power output, 32.4 mW at 84.98 GHz, being measured.

This was measured during test 2 and was achieved by applying a 4.5 V bias with a backshort length of 11.37 mm and no notch for the second harmonic backshort.

Repeating patterns for both the frequency and power are clearly visible during the testing of power and frequency output for different backshort lengths, as shown in figures 4.31 and 4.32.

Looking at the results from test 2 (figure 4.32), frequency dips and power peaks are noted at around 11.4 and 17.0 mm, marked as **A** and **B** on the graphs. This would indicate points where the signal reflected by the backshort intersects with the signal output from the diode with zero phase difference. The difference between the peaks is 5.6 mm and should be equal to the half wavelength of the RF signal, as calculated in equation 4.6. The calculated value of the half wavelength is $\frac{1}{2}\lambda_g = 5.63$ mm, and the difference between the calculated and experimental values is only 0.03 mm, so that would explain the power peaks.

The sudden change in frequency around these points is more complicated. The oscillator has been designed to resonate at the fundamental and second harmonic frequencies. In a system with multiple resonances, as the frequency approaches the point where the resonances cross, the frequency of oscillation will be pushed apart. As the two resonances cross, the frequency shoots to the other extreme, and slowly return to an approximately constant value once again.

4.3.5 Summary

Preliminary tests carried out at e2v demonstrated the system functioned in the desired way and produced a maximum output signal of 55 mW at 85.9 GHz. The system was then taken to UMIST where more detailed tests were carried out. Some of the measurement equipment was not calibrated but calculations suggest that the system will produce a higher output power signal than the e2v tests demonstrated.

Whilst we have been unable to influence the design of the multiple device oscillator with the results from the single diode oscillator, it does look like the calculations carried out in the design of the single device oscillator were correct, and match the operation of the device. The agreement between the single device oscillator design and function would suggest that the design of the multiple device oscillator, which is based on this single diode oscillator design, should also function as desired. Continuing with this design for the

multiple device oscillator should result in good power combining and the project aims being achieved.

Chapter 5

Multiple Gunn diode oscillator

5.1 Design

5.1.1 Introduction

Since testing of the single device oscillator began, adequate progress on the multiple device oscillator has been made, including the designs for the multiple device oscillator being submitted to e2v technologies for manufacturing.

The multiple device oscillator design is based on the single device oscillator design, the main difference is that three Gunn diodes are used in this design, so three diode housing sections must be manufactured. The three housing sections are all identical and based on the diode housing section in the single device oscillator. The project aims state that four diodes were going to be combined in the multiple device oscillator but due to a shortage of manufacturing time and improved Gunn diode performance, only three diodes will be combined. The target power of 100 mW using power combining should still be attained. The flow diagram in figure 5.1 illustrates how the components will now fit together.

5.1.2 Multiple device oscillator design

5.1.2.1 Second harmonic waveguide

The output waveguide, alternatively named the second harmonic waveguide, will be exactly the same in the multiple device oscillator as in the single device oscillator. The waveguide is designed to allow only the second harmonic

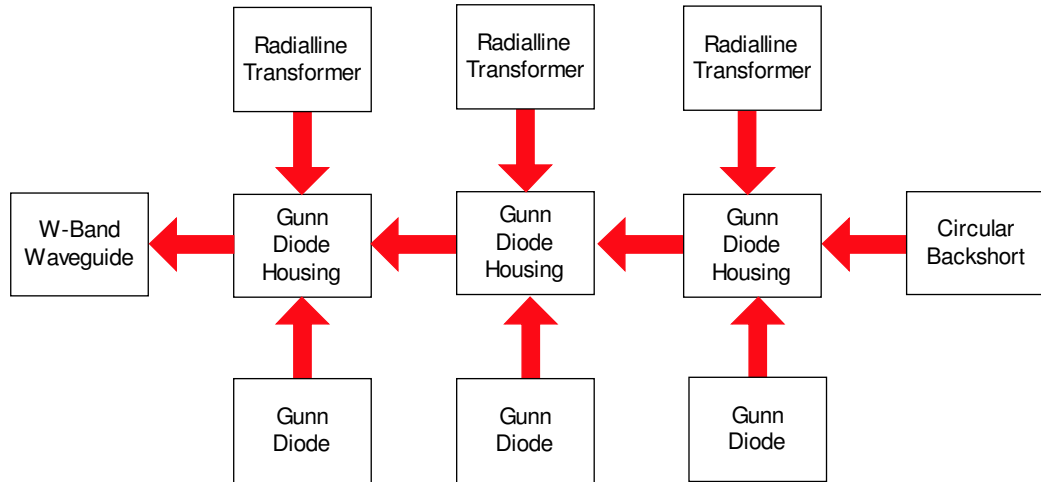


Figure 5.1: External components of the multiple device oscillator

through and reflect the fundamental back into the system. This component worked as expected with the single device oscillator therefore should continue to function correctly in the multiple device oscillator.

5.1.2.2 Gunn Diode Housing

The multiple device oscillator will enclose three Gunn diodes, the theory of the design has been obtained from the single device oscillator. Reviewing Barth’s paper for the in-line three diode combiner, it suggests “Power Combining at the fundamental frequency is a common technique and can be easily achieved with the present diode mount” (Barth 1981). Therefore the device measurements should be exactly the same as the single Gunn diode housing.

Figure 5.2 shows a sketch of Barth’s design using the three Gunn diode housings, this design can be used because it fulfils the condition $\lambda_g f_0 = 3\lambda_g f_{20}$ (Barth 1981). The design suggests that a frequency of 90 GHz with 60 mW of power is attainable.

The result of the single device oscillator was higher than expected at 85.9 GHz with 55 mW of power. Therefore it was suggested that three devices would be suitable instead of using four. If four devices were used, the internal heat generated would be greater than the individual Gunn diodes would be able to withstand.

After reviewing this multiple device oscillator design, one uncertainty that was raised was; how will all of the frequencies and powers of each diode

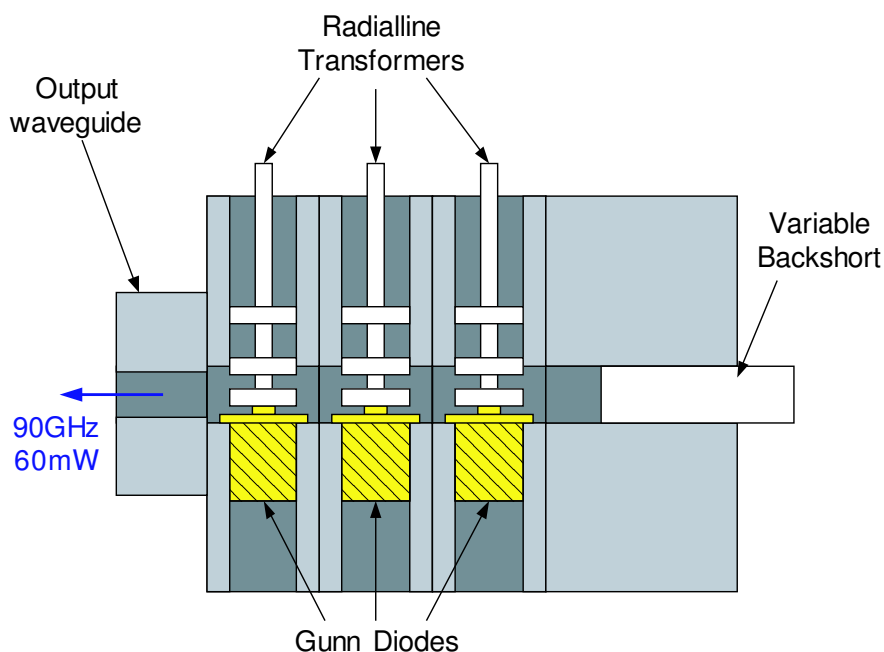


Figure 5.2: In-line three diode combiner

collectively combine? At this point it became apparent that Barth's paper may not be as good as it first appeared. The team questioned whether Barth had progressed as far as to manufacture the "in-line three diode combiner", since this practical issue of how the powers and frequencies combine is not commented upon in the paper.

This was a significant turning point in the project and two options became available. The first option was to mount the Gunn diodes exactly in the centre of each diode housing similar to the Barth design. The second option was to mount the Gunn diodes at a distance that would ensure that each diode was operating in phase with the other diodes, and this would result in the diodes not being positioned in the centre of the diode housing.

Evaluating both possibilities, the second option is the most favourable as the housing sections can be reversed or, if the diode position is different for each housing, the order of the housing section can be changed, which would give more variables to investigate during testing. An additional reason for choosing the second option is because the off-centre design is unique and may be the optimal solution to the power combining problem.

The next stage was to calculate the exact position for the Gunn diodes in the housing section. This was calculated based on the fact that the signal reflects

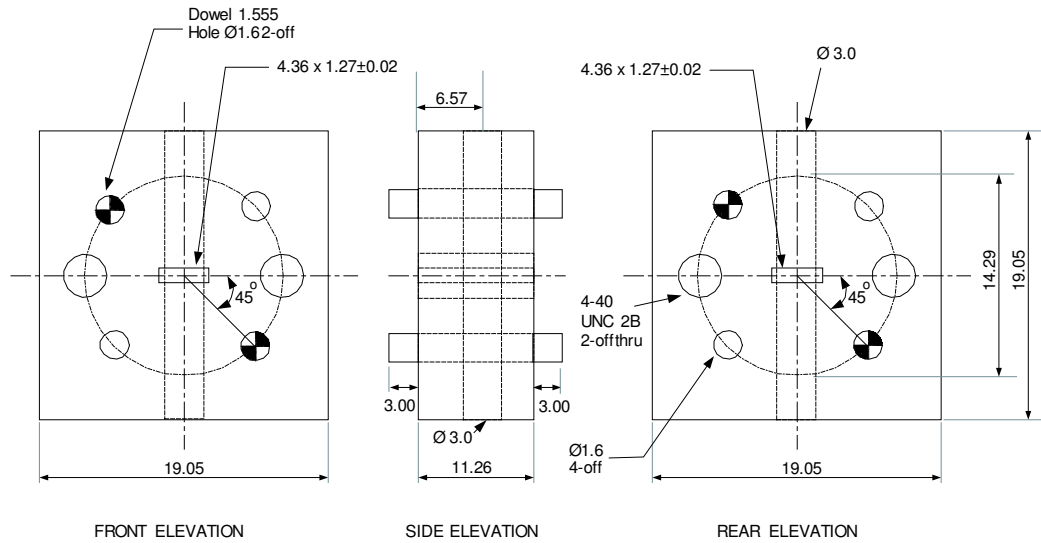


Figure 5.3: Gunn diode housing (Barth 1981)

against the waveguide cavity at 30° , which is approximately a twelfth of the guide length; 0.94 mm. This value is then added to the central mounting position and the correct mounting position becomes $5.36 + 0.94 = 6.57$ mm. Figure 5.3 shows the mechanical drawing of this component indicating the latest dimensions.

5.1.3 Backshort

The backshort housing will remain unchanged, though the backshort slide will be modified. One alteration that will be applied to the backshort slide is a screw which will clamp the backshort securely in position. This has an M3 thread and is attached approximately half way along the backshort housing.

5.1.4 Building progress

At this stage of the project the building is about six weeks behind schedule. The full set of mechanical drawings have been submitted to e2v and it is envisaged that the oscillator will be completed by the beginning of May, allowing time for testing.

5.1.5 Summary

The multiple diode oscillator is based upon the design of the single diode oscillator. Most of the system components remain the same though the position of the diodes in the diode housings and the backshort slide has been altered. The number of diodes in the oscillator has also been reduced from four to three diodes. The oscillator is currently being manufactured by e2v and should be complete by early May.

Looking back there could have been many different ways of tackling this section. Due to the lack of facilities available and significant turnover time for a single device, combined with the uncertainty of whether the device would operate correctly, this has caused a restriction on the types of experiments available. In an ideal situation it would have been possible to build several types of waveguide and experiment the effects of varying critical measurements.

5.2 Radial line transformer

The simulated RLT design from the single device will be used for the three RLTs to bias the Gunn diodes in the multiple device oscillator. Each of the RLTs will be manufactured to the same dimensions but will be tested with the diode inside the oscillator so that fine-tuning can take place. For this reason the RLT used for each diode will differ slightly as they are customised to suit a particular diode and section of cavity.

5.3 Power supply

5.3.1 Introduction

Due to manufacturing variations, each diode differs slightly from the others, resulting in the performance of each Gunn diode being unique. This means that the diodes may oscillate at different frequencies within the same waveguide structure at the same bias voltage. This effect was observed during testing of the single device Gunn diode oscillators provided by e2v technologies and the single device oscillator designed as part of this project. In order to power combine efficiently the diodes must lock frequency together and be in phase, meaning the frequency of each diode must be of the same magnitude and phase.

In a single device oscillator, the frequency can be tuned by altering the length of the backshort as well as the dimensions of the radial line transformer and Gunn diode. The frequency of oscillation can be tuned over a much smaller range by varying the bias voltage. However, the output power of the oscillator is also dependant on the bias voltage. In order to get the maximum power output at a specific frequency all these variables must be set.

The same variables which affect the output of the single device oscillator also affect the multiple device oscillator when power combining is to be achieved, as well as an additional variable. The distance between the individual Gunn diodes becomes important in the same way that the length of the backshort is important. It is envisaged that it will be difficult to alter the distance between the Gunn diodes over a continuous range like the alteration of the backshort length, therefore the ability to control the bias voltages of each Gunn diode becomes more important. It follows that it is important to have precise control of each diode bias voltage in the power combining oscillator to ensure that they oscillate at the same frequency and lock together.

During the testing of the single device oscillators, a linear 0–30 V, 2 A bench power supply was used. The advantage of this PSU is that it could be set to any bias voltage over the safe working range of the oscillator and supply sufficient current. In order to supply a multiple device oscillator a separate bench power supplies could be used for each Gunn diode. However, with the cost of a suitable linear bench power supply starting at £250, this is an expensive solution because four power supplies are required. It was decided that an alternative solution must be found.

The solution decided upon was to acquire one linear power supply capable of supplying the current for up to four Gunn diodes and then, using external circuitry, control up to four independent supply voltages.

5.3.2 Power supply requirements

The safe operating voltage limit for each diode is 6 V. The maximum current required by each Gunn diode at the point of switching the system on is almost 1 A. The bench power supply unit that was used during testing of the single device oscillator can only provide 2 A of current, which is not adequate for supplying up to four Gunn diodes. In the multiple device system only three diodes will be used, but the PSU will be created to supply up to four diodes due to the original project aims. This means that a new power supply is needed. The method of varying the voltage on the bench PSU was not easy to control with high accuracy; a small adjustment of the voltage control dial

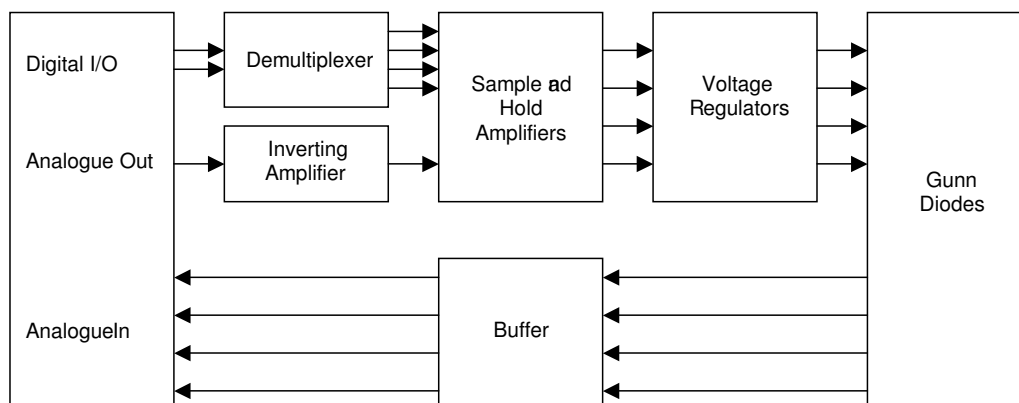


Figure 5.4: Hardware overview

could cause a large voltage change. This large change could be outside of the safe operating range and result in the destruction of the diode. So a finer adjustment of the voltage is desired.

A 7 V, 10 A fixed output linear power supply was acquired, which is suitable for the task. The voltage output of the PSU is fixed, so external circuitry is needed to create up to four adjustable voltages, one for each of the Gunn diodes. A simple solution to this would be to use a number of variable resistors to vary the voltage. For each output two variable resistors could be used; one for coarse adjustment and another for finer adjustment to prevent the sensitivity problem experienced with the bench power supply during testing of the single device oscillators. However, a much more precise method is preferred, a design which could also provide protection to the diodes if the current or voltage becomes too high. The use of a data acquisition board and some external circuitry would allow outputs to be precisely controlled by a computer and information to be fed back and displayed on screen. Figure 5.4 shown the hardware overview.

5.3.3 Data acquisition board

The data acquisition board used for the control of the power supply is a National Instruments Lab-PC+ ISA card. This is a low cost, analogue, digital, and timing I/O board for the PC. The Lab-PC+ board contains a 12-bit

successive approximation ADC with 8 analogue inputs, two 12-bit DACs for voltage output, 24 lines of digital I/O, and a 16-bit counter/timer. The wide range of inputs and outputs makes it ideal controlling the voltages to the Gunn diodes. The board has a 50-way I/O connector on the rear of the card which can easily be attached to the PCB containing the circuitry for the power supply.

The DAQ board supports a number of different programming languages, and even offers register level programming. The best supported method of programming is through a software package called LabView. This package is also made by National Instruments and links in well with the DAQ board. However, as the board is quite old in comparison to the software, so not all of the LabView functions are supported by the board, and the board documentation is quite limited.

5.3.4 Sample and hold

A sample and hold (S/H) amplifier is a circuit which will “hold” an output at a particular level even after the input signal has been removed. A simple form of the S/H circuit, as shown in figure 5.5, consists of two op-amps. The first op-amp, which accepts the input, acts as a voltage follower or unity gain buffer. This means that its output will follow whatever is fed into the input. This follower function works by negative feedback. This first op-amp provides a low output impedance which is vital for the next stage since it allows the capacitor to charge up to the input voltage very quickly once the digitally controlled switch is closed.

At the output there is another unity gain buffer enabling the voltage across the capacitor to be output. When the digital switch is open the voltage at the output will remain relatively constant because the op-amp has a very high input impedance so the capacitor does not discharge. Negative feedback further maintains the voltage. However, in practice the input impedance to the op-amp is not infinite, and also, due to leakage the capacitor will slowly lose its charge causing the voltage to drop. This drop in voltage is known as droop, and in order to minimise this, the S/H amplifier will need to be sampled regularly.

An IC has been chosen to perform the sample and hold operation. The SMP04 is a device made by Analog Devices and contains four sample and hold amplifiers within a single IC. “It has four internal precision buffer amplifiers and internal hold capacitors. It is manufactured in advanced oxide isolated CMOS technology to obtain high accuracy, low droop rate and fast

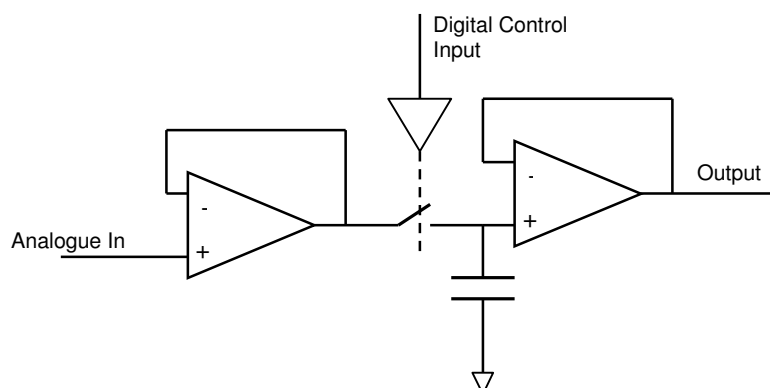


Figure 5.5: Sample and hold amplifier

acquisition time required by data acquisition” (Analog Devices 1998). The accuracy is specified to be 12-bit with a very low droop rate of 2 mV s^{-1} . This makes the SMP04 ideal for use in a wide range of applications. The use of this IC will minimise the number of separate components used, making troubleshooting any problems in the circuit a much simpler process.

5.3.5 Demultiplexer

Each of the S/H amplifiers in this IC are selected by a low input (active low) into the digital control pins. The DAQ board can provide a total of 24 digital outputs made up of 3 banks of 8. Four of these outputs can be used to address the four S/H amplifiers. However, this is an inefficient use of resources as this can be achieved by just using two of the digital I/O lines. Using two I/O lines will also make it much easier to program as only code for a simple binary counter will need to be created.

Truth table 5.1 shows which of the S/H amplifiers will be selected by the binary input signal from the DAQ board. Since only one analogue output from the DAQ is required at any given time, only one S/H amplifier will be active at any given time.

$$Q_1 = \overline{A.B} \quad Q_2 = \overline{A.\overline{B}} \quad Q_3 = \overline{\overline{A}.B} \quad Q_4 = \overline{\overline{A}.\overline{B}}$$

This solution can be implemented using a series of simple logic gates, as shown in figure 5.6.

The 74LS139 IC is a single chip solution which can carry out this function. This IC has been chosen, since its cost is lower than purchasing several logic

B	A	Q_1	Q_2	Q_3	Q_4
0	0	0	1	1	1
0	1	1	0	1	1
1	0	1	1	0	1
1	1	1	1	1	0

Table 5.1: Demultiplexer truth table

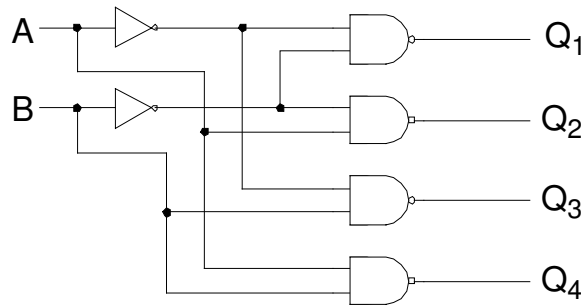


Figure 5.6: Line decoder logic

gate ICs, it reduces the external circuitry and will make fault checking easier.

5.3.6 Inverting amplifier

The voltage regulator requires the use of a negative reference voltage, but as the DAQ board is only able to supply a voltage in the range of 0-10V an inverting amplifier will be required to invert the voltage, as shown in figure 5.7. This amplifier should have a gain of -1. A different gain would result in the voltage value entered into the computer differing from the bias voltage applied to the diodes.

The gain is calculated as $-\frac{R_f}{R_i}$, therefore for a gain of -1, R_f must equal R_i . Two $1\text{ k}\Omega$ resistors have been chosen for these.

5.3.7 Buffer

The Gunn diodes have a considerable amount of current flowing through them, in the region of almost 1 A. In order to prevent this current flowing into data acquisition board and damaging the board, some isolation is required.

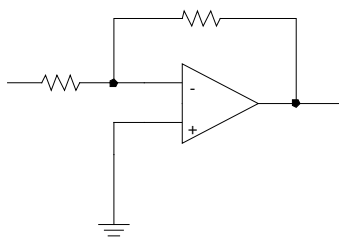


Figure 5.7: Inverting amplifier

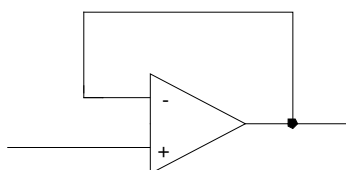


Figure 5.8: Voltage follower

A simple voltage follower circuit comprising of an op-amp using negative feedback can be used, as shown in figure 5.8. The op-amp provides a high input impedance to prevent this reverse current flowing, and the negative feedback makes it act as a unity gain buffer so the output voltage follows the input voltage.

5.3.8 Voltage regulator

In order to independently regulate the four separate outputs of the PSU, four individual 723 voltage regulator integrated circuits with pass transistors will be used. These are an inexpensive way to provide a high current output at a set reference voltage. The reference voltage is set by the data acquisition board via the sample and hold circuitry. The 723 regulator also allows current limiting to be put in place to prevent damage to the power supply and pass transistors if the outputs become short circuited.

The basic schematic of the 723 voltage regulator is shown in figure 5.9.

The 723 regulator comprises a number of basic components: a differential amplifier with an output transistor and a current limiting transistor. With the use of external circuitry this integrated circuit can provide the specifications stated above.

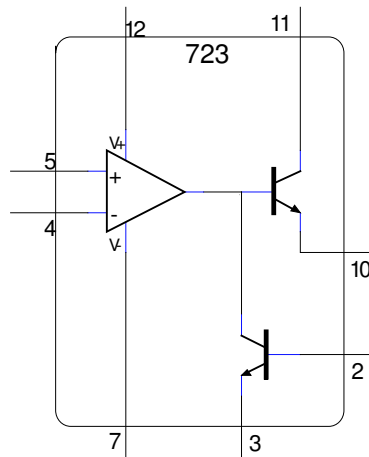


Figure 5.9: 723 Regulator

Figure 5.10 shows the 723 voltage regulator with the required external circuitry.

5.3.8.1 Operation

- The 7 V DC voltage is provided by the fixed voltage power supply unit and is capable of sourcing up to 10 A.
- The +12 V and -12 V voltages are control voltages provided by the data acquisition board and used to control the external circuitry.
- The non-inverting input of the integrated differential amplifier (pin 5) is held at ground potential to provide a stable reference point.
- If resistors R_2 and R_3 have the same resistance then they form a potential divider between V_{in} and V_{out} connected to the inverting input (pin 4). As, under normal operation conditions, this pin will be held at a virtual ground potential it can be seen that the relationship between the input and output voltages will be $V_{out} = -V_{in}$.
- The 723 can only supply a maximum of 150 mA at its output (pin 10) so an external pass transistor is used to provide the current required by the Gunn diodes.
- Resistor R_1 is used as a current limiting resistor. As the output current increases, so will the voltage across resistor R_1 . If the voltage across

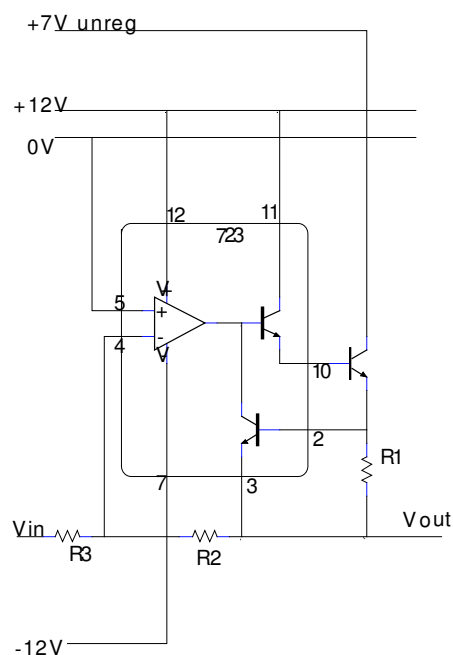


Figure 5.10: Setup of the 723 voltage regulator

R_1 reaches a point where the base-emitter (pin 2-pin 3) junction of the current limiting transistor becomes forward biased to turn on this transistor then the output voltage will be reduced automatically, thus limiting the output current. The turn on voltage for the current limiting transistor is approximately 0.5 V.

5.3.8.2 Calculating component values

R_1 : This resistor will have a voltage drop across it when the output current is at a maximum. If the maximum output current is limited to 1.5 A then the value of resistance may be calculated using ohms law:

$$R_1 = \frac{V_{drop}}{I_{max}} = \frac{0.5V}{1.5A} = 0.33 \Omega \quad (5.1)$$

The maximum heat dissipation in this resistor will be:

$$P_{diss} = I_{max} V_{drop} = 1.5A \times 0.5V = 0.75 W \quad (5.2)$$

R_2, R_3 : As these resistors provide the feedback to control the output voltage from the reference input voltage, they should not overload the

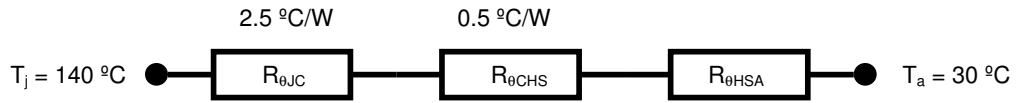


Figure 5.11: Thermal circuit of the pass transistor under fault conditions

sample and hold circuitry. Resistances of $10\text{ k}\Omega$ will draw a feedback current of less than 1 mA .

Q_1 : The external pass transistor is chosen to be capable of carrying the required 1.5 A maximum output current whilst capable of dissipating all of the heat generated if a short circuit occurs. To dissipate this heat, the device must be mounted on a heat sink. The device chosen is the D44H11 NPN transistor manufactured by Motorola. This device was chosen based on its package design, capabilities, price and availability.

The maximum continuous collector current of this device is 10 A . This is much more than that required by the system. Each device costs $\pounds 0.84$ and comes in a TO220 package which is readily mounted to a heat sink.

In short circuit conditions the transistor will have a maximum collector current of 1.5 A while the voltage across the collector and emitter may be as high as the supply voltage, 7 V , minus the voltage drop across the limiting resistor. This means that the maximum power that the transistor must dissipate will be:

$$P_{diss} = I_{max}V_{drop} = 1.5\text{ A} \times (7 - 0.5)\text{ V} = 9.75\text{ W} \quad (5.3)$$

The thermal circuit shown in figure 5.11 may be used to calculate the value of heat sink required.

Where:

T_j	Maximum desirable temperature of the junction.
T_a	Maximum ambient temperature.
$R_{\theta JC}$	Thermal resistance between the junction and the case.
$R_{\theta CHS}$	Estimate of the thermal resistance between the case and the heat sink.

$R_{\theta HSA}$ Thermal resistance between the heat sink and the ambient temperature.

With the analogy to ohms law, the heat flow can be calculated using $\Delta T = P \times R$. The maximum dissipated heat is 9.75 W then $P = 9.75$ W and the difference in temperature (ΔT) is $140 - 30 = 110^\circ\text{C}$.

Therefore:

$$\begin{aligned}\Delta T &= P(R_{\theta JC} + R_{\theta CHS} + R_{\theta HSA}) \\ 110 &= 9.75(2.5 + 0.5 + R_{\theta HSA}) \\ R_{\theta HSA} &= 8.28^\circ\text{C W}^{-1}\end{aligned}\tag{5.4}$$

The heat sinks chosen are designed to fit the transistor TO220 package and have a thermal resistance of 8.6°C W^{-1} .

C_1 : This capacitor is a 560 pF ceramic capacitor connected between pins 4 and 13 as recommended on the data sheet by the manufacturer.

C_2 : This is designed to give a low output impedance at high frequencies. $10\ \mu\text{F}$ is considered as adequate for this.

5.3.8.3 Four output design

The 723 IC voltage regulator circuit discussed above forms the basic building block for providing up to four individually controlled outputs. Figure 5.12 shows the four output regulator.

5.3.8.4 Component list

C_1 560 pF ceramic disc capacitor.

C_2 16 V $10\ \mu\text{F}$ tantalum capacitor.

Q_1 D44H11 NPN complementary silicon power transistor, Motorola.

R_1 $3 \times$ parallel $1\ \Omega$ wire wound resistor.

R_2, R_3 $10\ \text{k}\Omega$ metal film resistor.

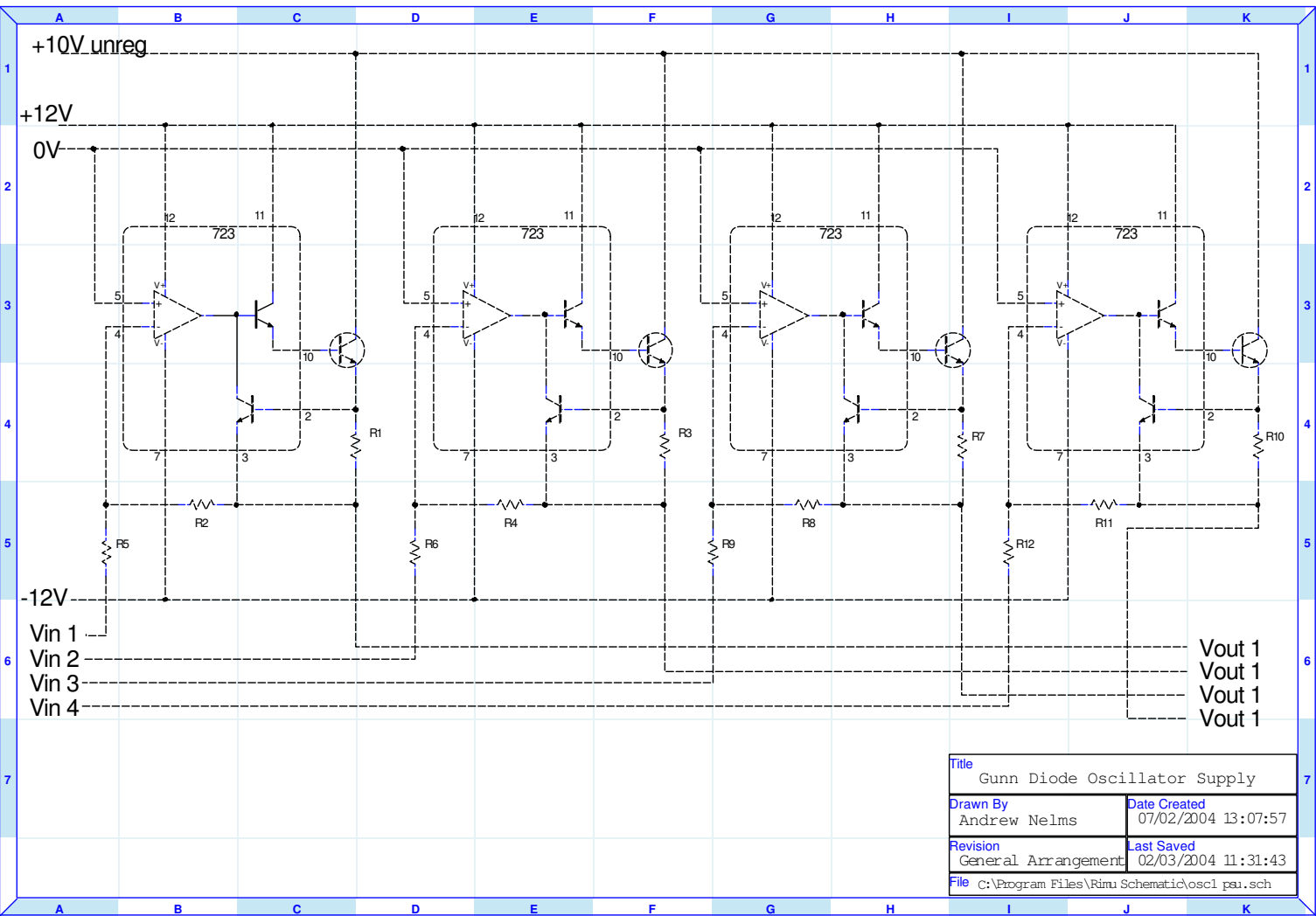


Figure 5.12: Four output regulator

5.3.9 LabView

LabView is a graphical development environment designed for measurement, control, and automation of systems. LabView allows complex measurement, control and automation control applications to be made relatively quickly and easily. Unlike general programming languages such as C or Assembly, LabView is designed specifically for these needs meaning that powerful applications can be created without the need to learn these very complex programming languages. With LabView, programs can be made by connecting a sequence of blocks together with “wires”, where each block carries out a particular function, there is no need to write out lines of code.

The program structure is top down like in C, and LabView works from left to right. Many functions that are found in C are also implemented within LabView such as “for loops”, “while loops”, and “if statements”. LabView offers support for hundreds of instruments and measurement devices through the use of virtual instruments, VIs, giving the ability for these devices to be quickly configured ready for use. LabView can create an instrument panel for this device providing easily accessible controls and a range of readings. These controls can be in the form of switches, dials or input boxes, and the readings can be in the form of graphs, charts or a numerical display. These functions make it an ideal tool for creating a control program for the PSU for the multiple device oscillator.

The aim of the program is to enable a user to set four individual voltages on the computer and for each of these set voltages to be output to a diode within the multiple diode oscillator. As the data acquisition board does not have enough analogue outputs, the circuit which has been designed takes a single analogue output together with two digital outputs and creates four analogue outputs from this, as described in section 5.3.5. To achieve this, the LabView program will need to control the data acquisition board so that a particular analogue value is only output when the corresponding sample and hold amplifier is selected.

The program, shown in figure 5.13 is a “while loop”, and all of the elements in the figure are enclosed within the loop which will repeat indefinitely, or until the stop button is pressed on the instrument panel. Within this “while loop” is a “for loop” which increments the iteration “count, i , from 0 up to 3 and reset when it reaches 4”. This is connected to the “write to digital port” virtual instrument (VI) so the value of the iteration will be output as a binary value to the circuit.

The iteration “count” is also connected to an “index array” function. This function acts in the same way as a multiplexer and selects the corresponding

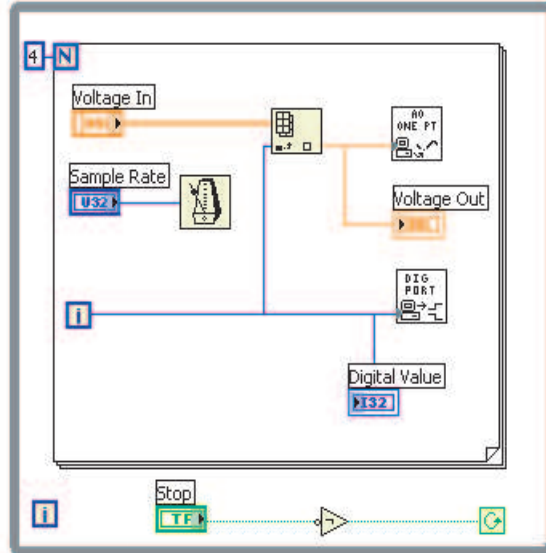


Figure 5.13: Initial program

analogue voltage from the array that is specified on the instrument panel. The selected analogue value is then written to the analogue out port using the “AO update channel” VI. Therefore, each of the four analogue voltages that are specified on the instrument panel will have a different digital value. This means that for each of the voltages, a different sample and hold amplifier will be selected allowing four individual analogue outputs to be created. Within the “for loop” there is also a “delay” function which allows the sample rate to be adjusted by the user. Using a fast sample rate, droop can be minimised, but the sample rate must not be too fast that the voltage across the hold capacitance does not reach the input voltage.

The data sheet for the sample and hold amplifiers’ state that the droop is 2 mV s^{-1} , and the slew rate is $4 \text{ V } \mu\text{s}^{-1}$ (Analog Devices 1998). Voltages up to 6 V are required, so this rate must be slower than once every $1.5 \mu\text{s}$, but faster than 0.5 s to prevent a droop of more than 1 mV . The sample rate can be adjusted relatively easily, so once the power supply is completed an appropriate rate can be chosen.

Using this initial program as a basis, a second program was created to enable more automation and control. It is desirable to be able to ramp up the voltage gradually, since a sudden change in the voltage, for example 0 V straight up

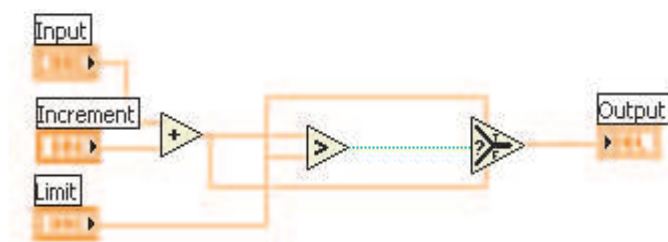


Figure 5.14: Increment VI

to 6 V, can destroy the Gunn diode. A simple sub VI was created to perform an increment function; this is shown in figure 5.14.

This virtual instrument takes the “input” value and adds it together with the “increment” value. This new value is then compared with the “limit” which is the value it should ramp up to. If the new value is less, the new value is output. Otherwise the “limit” value will be output.

This VI was then placed within the main program and a number of modifications were made to accommodate this function. When the program is run the voltages are all initially set to zero. The voltage is then incremented by the VI. This voltage incrementation is done simultaneously for all four voltages, and the outputs are passed into shift registers at the edge of the “for loop”, and a “build array” function. The “build array” function creates an array of voltages, and as with the initial program, the iteration count will select the corresponding voltage to be output. The shift register will pass the value to the start ready to be incremented again. A reset feature has also been added so when the reset on the instrument panel is pressed a 0 will be passed into the “increment” VI instead of the value in the shift register. The final program is shown in figure 5.15.

Figure 5.16 shows an example of the instrument panel. All of the values can easily be set using the arrows at the side of the boxes, or by entering a value directly into the text box. The reset controls are a set of switches and can be activated by a simple click. These reset switches light up to demonstrate that they have been pressed, like an electronic switch. The displays at the bottom of the panel show the voltage that is being output at the analogue output, and the decimal value of the digital outputs of the data acquisition board.

The voltages at the analogue inputs are measured using the “AI update chan-

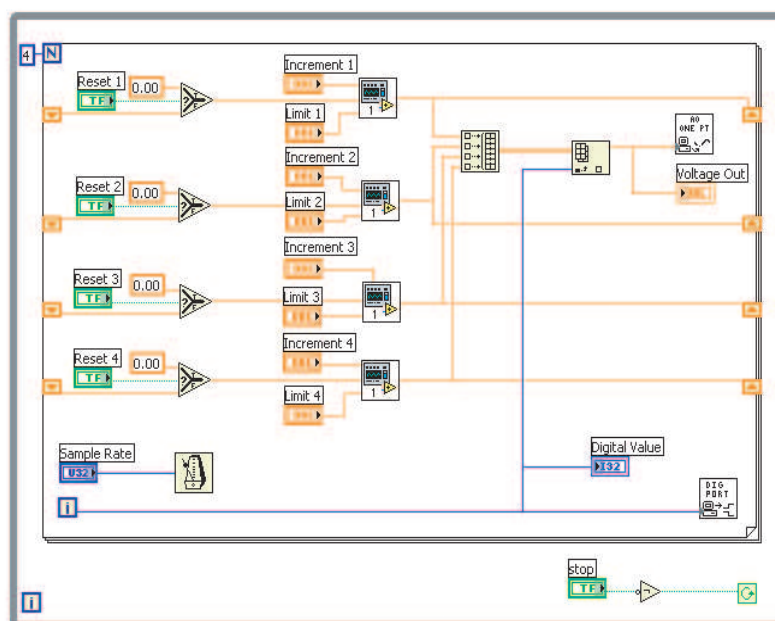


Figure 5.15: Revised program

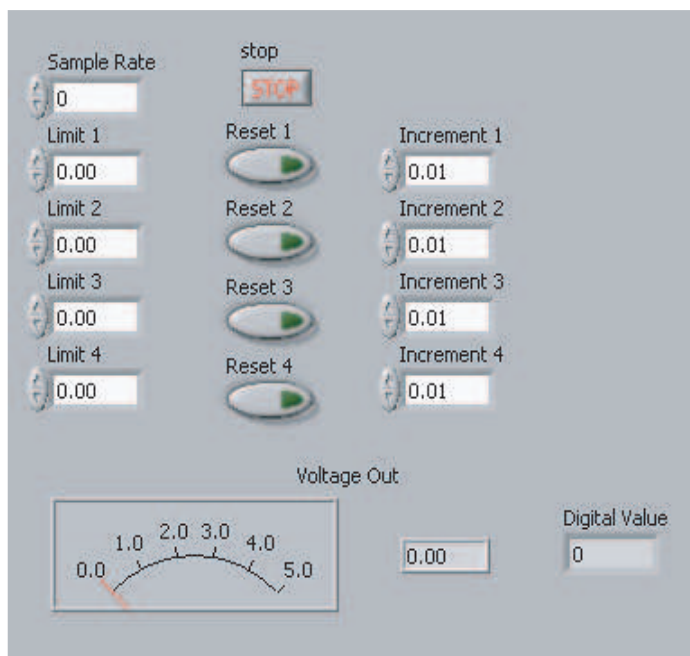


Figure 5.16: Instrument panel

nel” VI. The channel terminal is used to select which analogue input should be read. Taking the difference between the two analogue inputs from across the current limiting resistors, and dividing by this resistance value, the current can be calculated and displayed on the instrument panel. The current through the resistor is the same as the current through the Gunn diode. Therefore, the power in can be calculated, and the DC to RF efficiency can be worked out using the power out from the spectrum analyser.

5.3.10 Summary

A PSU to provide independent voltages is required to optimise the system’s performance to help ensure the Gunn diodes oscillate at similar frequencies to efficiently lock together. There are a number of ways the independent voltages could be created, but the chosen method is to use a linear power supply unit combined with a data acquisition board, set and controlled by a LabView program.

The result is the creation of a power supply unit that has four independent and digitally controlled voltage supplies, with voltage and current regulation. The properties of the unit are easy to control using a computer and the unit’s performance can be monitored in a similar way.

Chapter 6

Conclusions

6.1 Progress to date

From October until the beginning of November the team spent all of the project time researching Gunn diodes, their physics, uses and previous research and designs, as well as looking at housings and power combining techniques. The findings were presented to e2v Technologies. At this meeting, e2v defined the project aims and gave additional direction to the project, advising against the use of planar housing and indium phosphide (InP) Gunn diodes.

It was decided that gallium arsenide (GaAs) Gunn diodes would be used and placed inside a waveguide housing. Half of the team began to learn to use the simulation tools ADS and HFSS. The second half of the team continued to do research, looking at waveguide housing, and beginning the design of the single Gunn diode system. At this time, mid November, work began on the Interim Report, which was handed in on 19 December. The designs for the single Gunn diode system were submitted to the UMIST workshop at the same time, and the completion date the workshop offered for the system to be manufactured was mid-January. All of the work up to this point is documented in the Interim Report.

In January the UMIST workshop contacted the team to return the designs, explaining they were unable to manufacture the system to the required standard; manufacturing tolerances of 0.02 mm. After research into other possible manufacturers the designs were passed to e2v. This caused the project to be delayed by seven weeks.

The original objective was to build and test the single Gunn diode system and, if it functioned correctly, base the design of the multiple Gunn diode

system on it. The new objective became; assume that the single Gunn diode system functions correctly and continue with the project as planned, basing the multiple Gunn diode system on the single Gunn diode system design. This change was an endeavour to reduce the delay to the project. The new plan held huge risk; if the single Gunn diode system did not work, the multiple Gunn diode system would have to be redesigned, which could result in the multiple Gunn diode system not being manufactured before the project submission date.

On 23 March the team went to e2v to collect the completed single Gunn diode system. At the e2v site, the team began preliminary tests on the system, demonstrating it functioned correctly and better than expected, the output signal was 85 GHz with 55 mW of power. e2v spent some time working with the team to optimise the system's behaviour and carry out the testing process.

The designs for the multiple Gunn diode system were submitted to e2v at this time, and a number of issues with the design were discussed and settled. The system should be manufactured by May; this is six weeks behind the time plan. e2v have offered help with testing and optimising the multiple Gunn diode system to enable the project to be completed on time. After discussions with e2v, it was decided to reduce the number of diodes being combined in the multiple Gunn diode system. It was suggested to combine three diodes instead of four; since three diodes will be sufficient to prove whether power combining has been achieved and should be able to attain the desired power, 100 mW.

Currently, simulation work is still ongoing, particularly in the optimisation of the radial line transformer. The single Gunn diode system is being tested and research is being completed into further work and other projects that could be done after this project to complement its findings.

In summary, the project is currently behind schedule by six weeks, but because extra time was written into the original time plan and e2v have offered advice and some help, the project should be completed on time. There is only one change in the aims, and that is to power combine three Gunn diodes instead of four.

6.2 Future objectives for this design

Work is on-going to meet the project aims but once these aims are met there are a number of additional objectives that would enhance the findings of the

project. These objectives are not going to be completed as part of this project, though they may be a good starting point for another team to continue the research and optimisation of Gunn diodes using power combining.

6.2.1 Simulation of the backshort

Different types of backshort design were created and their losses were calculated. It would be interesting to simulate the different types of backshorts and compare their affect on the system, as well as using the simulation to observe the magnitude of the losses due to each backshort design.

Tests of the single device oscillator have illustrated that the position of the backshort affects the performance of the system. HFSS could be used simulate the backshort in both of the oscillators and study the effect of varying the backshort position. These results could then be compared to the experimental results obtained.

6.2.2 Simulation of the diode position

To optimise frequency locking, the diodes are not positioned in the centre of the diode housing sections in the multiple device oscillator. The position has been mathematically calculated and the simulation package HFSS could be used to verify the position of each diode and the spacing required between each of the Gunn diodes, as described in section 5.1.2.2.

HFSS could also be used to study the effect of the different waves that are produced by the Gunn diodes and study how they interact with each other in the waveguide cavity.

6.2.3 Alternate waveguide designs

It was calculated that the attenuation and Q -factor of the circular backshort was best; lowest attenuation and highest Q -factor, in comparison to the rectangular waveguide. It would be interesting to redesign the system using circular waveguide throughout the design and verify if this is true. This verification could be completed by simulation or manufacturing and testing the system.

6.2.4 Power combining more Gunn diodes

The original aim of the project was to power combine four diodes but due to time constraints this was changed to three diodes. It would be interesting to investigate the combining of four diodes and comparing the results of the two oscillators, particularly considering whether frequency locking is harder to achieve with more diodes and whether the power output increases by a third, due to their being a third more diodes, or if the efficiency is reduced as the number of diodes increases.

In addition to considering a four-diode oscillator, it would also be interesting to try to combine a larger number of diodes.

6.2.5 Power combining at non-fundamental harmonics

The power combining of both of the oscillators was achieved at the fundamental frequency since research by Barth suggested this method was achievable. Power combining at the second, or any other harmonic may also be possible and this could result in system optimisation, particularly because the efficiency of the system may be affected.

Chapter 7

Future work

Many groups, including UMIST and e2v, are interested in optimising the performance of Gunn diodes and Gunn oscillators. The research completed in this project is a starting point to achieve this optimisation. There is a suggestion for further work that could be completed to complement this project.

7.1 Hot electron injection

7.1.1 Reasons for hot electron injection

Hot electron injection allows electrons to be injected into a device through a narrow GaAs base region without significant relaxation. (Beton, Long, Couch & Kelly 1988). Traditionally, without hot electron injection, the energy of electrons is increased to the X band through large electric fields in the start of the drift zone. The area where this happens is a region which does not allow domain formation, and is known as the dead zone. The formation of the dead zone reduces the effective drift region length and acts as a parasitic resistance, reducing device efficiency (Neylon, Dale, Spooner, Worley, Couch, Knight & Ondria 1989).

Hot electron injection is the process of raising the energy of an electron into the X band before it enters the drift zone. This can be achieved by creating very large electric fields inside the semiconductor itself. In theory, Schottky barriers could be used, but there are problems with the metal-semiconductor interfaces. Planar doped barriers and graded gaps can be used more practically.

Using such techniques brings with it an additional benefit. The temperature of the electrons travelling across the junction will be set by the electron energy. This is typically equivalent to around 2000 K, so variances of 130 K required for the full military specifications will have relatively little impact (Neylon et al. 1989).

Hot electron injection is achieved by creating a heterojunction at the cathode of the diode. Generally, this is a layer of AlGaAs between the cathode contact and the active area. The electrons will gain energy when crossing this junction. An energy gain of around 0.25 eV is expected for Al_{0.3}Ga_{0.7}As layers. A significant proportion of electrons will be transferred from the Γ valley to the X valley because of this (van Zyl, Perold & Botha 1999).

Since this effectively reduces the dead zone, the RF power output of the device is increased. Also, smaller active areas can be created, allowing higher fundamental frequencies to be achieved.

7.1.2 Experimental results

During initial work on hot electron injection, 80 mW of power was achieved at 90 GHz with an efficiency of 2.4%. 50–60 mW at 94 GHz achieved reproducibly, giving a 1.6% efficiency on conversion from DC to RF power. It was theorised that with further enhancements such as grading the drift region to engineer the electric field throughout the device and placing the injector at the cathode, closer to the heatsink, that powers of 100 mW at 94 GHz could be achievable (Neylon et al. 1989).

After the publication of this paper, most people placed the injector at the cathode of the diode. Since then, diodes have been fabricated with multiple transit regions and multiple hot electron injection points. This effectively created multiple hot electron injection diodes in a single physical device. With this arrangements, RF powers of 160–178 mW were achieved at 73 GHz (van Zyl et al. 1999). Power combining with such devices could potentially result in very high power outputs from an oscillator, possibly 450 mW at 87 GHz when combining three diodes.

Appendix A

Electronic information

This section provides various digital documents that may be of interest to the reader. In order to view this appendix, place the included CD into an appropriate drive in your computer. If your computer is set to use Windows Autoplay, the menu should be loaded automatically. If not, please follow these steps to load the menu:

Windows 95 or above including NT

1. Insert the CD into an appropriate drive.
2. Click the Start button.
3. Choose Run.
4. In the resulting dialog box, type `D:\index.html` replacing D with the letter of your CD drive.

Other operating systems

1. Insert the CD into an appropriate drive.
2. If required, mount the CD.
3. Start a web browser.
4. Enter the following URL: `file:///path-to-cd/index.html` where `path-to-cd` should be replaced with the actual path to the CD for your operating system and hardware.

A.1 Project plan

Planning is important for any project, especially so for a long-term project such as this one. Careful attention was paid to the project time plan, copies of which are available on the attached CD.

A.2 Records of the meetings

As the project was progressing, regular meetings were organised between the team members and the supervisors. Agendas were created for these meetings, and minutes were recorded for reference. These documents can be found organised chronologically on the attached CD.

A.3 Financial accounts

A copy of the accounts for the project is available on the attached CD.

A.4 Presentation slides

A presentation was organised to allow us to demonstrate to e2v Technologies the current level of our understanding of the project and discuss the aims and objectives for the project. It was also designed to introduce the project team and set the scene for some questions to be asked. The slides used in the presentation are available on the attached CD, as are the slides used for the formal project presentation in January.

A.5 PHP source

Source listings for the PHP scripts used to create the project web site are included on the attached CD. Discussion of why PHP is used in the site is provided in the interim report. Web site changes this semester are discussed in section 3.4 of this report.

A.6 Technical drawings

Mechanical drawings for various methods of waveguide construction are provided in this section.

A.7 Issues log

A log was maintained containing all issues that arose during the project to track their progress and ensure resolution. A copy of this log is available for viewing in this section.

A.8 Experimental results

Raw data from the testing of the oscillators is presented in this section.

A.9 Communications log

A log of all communications with e2v was created to help to facilitate a professional relationship between the team and e2v, and avoid excessive contact that may waste everybody's time. This log is available for viewing in this section.

A.10 Power supply

The schematic and PCB layout for the power supply unit for the multiple device oscillator is available for viewing here, along with information on the LabView modules used to build the control interface to the PSU.

A.11 Main reports

A copy of this report and the interim report are also included on the attached CD for reference.

Bibliography

Analog Devices (1998), ‘SMP04 CMOS quad sample and hold amplifier datasheet’. Accessed 2 April 2004.

*http://www.analog.com/UploadedFiles/Data_Sheets/1172124SMP-04_d.pdf

Barth, H. (1981), A wideband, backshort-tunable second harmonic w-band Gunn-oscillator, *in* ‘MTT-S International Microwave Symposium Digest’, Vol. 81, IEEE, pp. 334–337.

Beton, P. H., Long, A. P., Couch, N. R. & Kelly, M. J. (1988), ‘Use of n+ spike doping regions as nonequilibrium connectors’, *IEEE Electronics Letters* **24**(7), 434–435.

Ferry, D. K. & Grondin, R. O. (1985), *Transport in Submicrometer Devices*, Vol. 9 of *VLSI Electronics*, chapter 12, pp. 421–440.

Gunn, J. B. (1963), ‘Microwave oscillations of current in III-V semiconductors’, *Solid State Communications* **1**, 88–89. Supplement to the Journal of the Physics and Chemistry of Solids.

Holzman, E. L. & Robertson, R. S. (1992), *Solid-State Microwave Power Oscillator Design*, first edn, Artech House, Inc.

Matthai, G., Young, L. & Jones, E. M. T. (1980), *Microwave filters, impedance-matching networks and coupling structures*, McGraw-Hill.

Neylon, S., Dale, I., Spooner, H., Worley, D., Couch, N., Knight, D. & Ondria, J. (1989), ‘State-of-the-art performance millimetre wave gallium arsenide Gunn diodes using ballistically hot electron injectors’, *IEEE MTT-S Digest* pp. 519–522.

Pozar, D. (1998), *Microwave Engineering*, second edn, John Wiley.

Reiss, G. (2001), *Project Management Demystified*, second edn, Spon Press.

The Electricity at Work Regulations (1989). London, HMSO.

van Zyl, R. R., Perold, W. J. & Botha, R. (1999), Multi-domain Gunn diodes with multiple hot electron launchers: A new approach to mm wave GaAs Gunn oscillator optimization, *in* 'Africon', Vol. 2, IEEE, pp. 1193–1196.